Disclaimer

This note has not been internally reviewed by the DØ Collaboration. Results or plots contained in this note were only intended for internal documentation by the authors of the note and they are not approved as scientific results by either the authors or the DØ Collaboration. All approved scientific results of the DØ Collaboration have been published as internally reviewed Conference Notes or in peer reviewed journals.

DØ NOTE 1381

DOE Dist. Cat. UC-414

LBL-33748
March 1993

Experimental Techniques for *B* Physics

Natalie A. Roe

Physics Division
Lawrence Berkeley Laboratory*
University of California
Berkeley, California 94720

Lectures Presented at the
SLAC Summer Institute
July 13-24, 1992

*This work was supported by the Director, Office of Energy Research, Office of High Energy and Nuclear Physics, High Energy Physics Division, of the U.S. Department of Energy under Contract No. DE-AC03-76SF00098.

Experimental Techniques for B Physics

Natalie A. Roe
Lawrence Berkeley Laboratory

1 Introduction

In recent years, interest in B-meson physics has been increasing steadily, as evidenced by increases in the annual publication rate. This is illustrated in Fig. 1, which shows the annual number of publications (taken from the Spires database) in B-meson physics and Υ physics since 1977, the year of the discovery of the Υ. Interest in Υ physics peaked a few years after its discovery and has since waned, while the trend in B physics is still upward. Why does B physics still hold such fascination for us, more than 10 years after the initial discovery of the B_d and B_u mesons?

There are several factors behind the sustained growth in the field of B physics. First of all, B's decay weakly, giving us an opportunity to probe the CKM matrix. This will be discussed in more detail in the next section. Secondly, the b quark is heavy; therefore, perturbative calculations of its decays should be more reliable, and experimental measurements should provide a real test of the theory. The fact that the b quark is heavy is also important experimentally, because a significant amount of energy is released when it decays to the much lighter c quark. This allows b quarks to be identified by looking for energetic leptons, for example. Thirdly, the B's have a relatively long lifetime. This came as somewhat of a surprise when it was first measured in 1983 at PEP [1]. The lifetime is long enough to be directly observed, and it can be used as a tag for b quark decays. Fourthly, due to the large top quark mass, B's have a relatively large mixing rate; the first evidence for this came in 1987 from the UA1[2] and ARGUS [3] experiments. The mixing diagrams give us another opportunity to determine some of the parameters of the CKM matrix.

The large mixing rate in the $B\bar{B}$ system has another important ramification: interference between direct decay to a CP eigenstate and mixing

This work was supported by the Director, Office of Energy Research, Office of High Energy and Nuclear Physics, Division of High Energy Physics, of the U.S. Department of Energy under Contract No. DE-AC03-76SF00098.

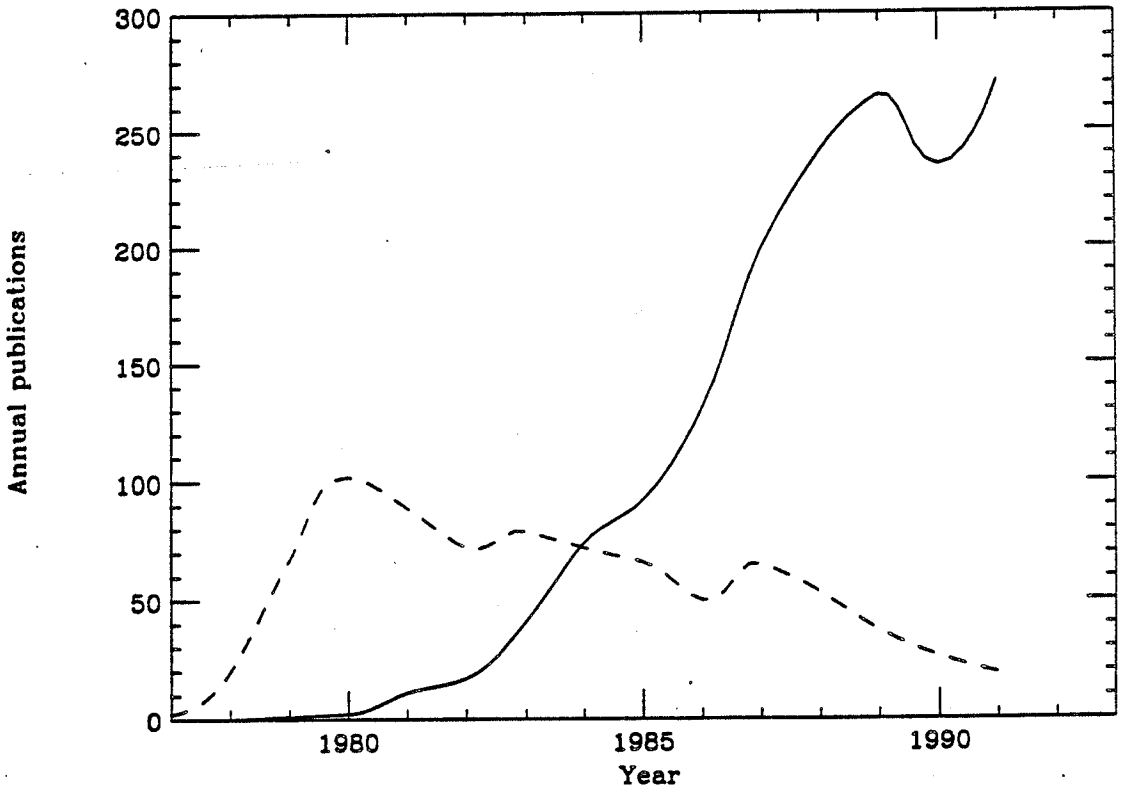

Figure 1: Publications per year in B physics (solid) and Υ physics (dashed).

followed by decay to a CP eigenstate can result in observable rates of CP violation in B-meson decays. The realization that nature may have provided us with another system to probe CP violation (in addition to the neutral K mesons) has greatly contributed to the interest in B physics, and resulted in many proposals all over the world to build dedicated B 'factories' to search for and study CP violation in B decays.

In these lectures I will try to give an overview of the field of B physics, beginning with a short introduction to the theory of B decays. I will then describe the B meson production properties and experimental techniques at a variety of accelerators, including e^+e^- colliders operating on the $\Upsilon(4S)$, in the continuum, and at the Z^0, as well as at hadron colliders and fixed target experiments. Finally, I will give a selective overview of experimental measurements in B physics, without any pretense at being comprehensive. I will not discuss the very interesting subject of CP violation in the B system, but instead refer the reader to the lectures in this series by Yosi Nir and Harry Nelson on, respectively, the theoretical and experimental aspects of CP violation.

2 B Decays in the Standard Model

In the Standard Model of particle interactions, charged weak decays are not flavor-conserving, as illustrated in Fig. 2. The weak eigenstates are therefore not identical with the flavor eigenstates, and by convention we normally rotate the down-type quarks in order to obtain the weak eigenstates. This rotation is described by the Cabibbo-Kobayishi-Moskawa (CKM) matrix, a complex, unitary 3x3 matrix. The nine elements of the CKM matrix are denoted by $V_{qq'}$, where q runs over the up-type quarks u, c, t and q' runs over the down-type quarks d, s, b. The charged weak current couples an up-type quark to a down-type quark with an amplitude given by $V_{qq'}$. The 18 parameters of this complex 3x3 matrix can be reduced to four, consisting of three angles and one phase, when one applies unitarity and eliminates redundant phase rotations. The phase is important because it makes CP violation possible within the Standard Model.

The CKM parameters are not predicted by the theory, but are fundamental parameters of the 3-generation Standard Model and must be experimentally determined. By measuring each element $V_{qq'}$ independently we can test unitarity and determine whether all couplings are consistent with the 3-generation CKM matrix. In addition, one would like to make a definitive test to determine whether CP violation is due to the CKM phase or is due to some form of new physics.

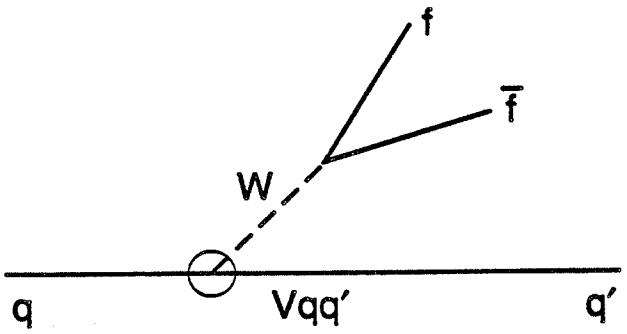

$$\begin{pmatrix} d' \\ s' \\ b' \end{pmatrix} = \begin{pmatrix} V_{ud} & V_{us} & V_{ub} \\ V_{cd} & V_{cs} & V_{cb} \\ V_{td} & V_{ts} & V_{tb} \end{pmatrix} \begin{pmatrix} d \\ s \\ b \end{pmatrix}$$

XBL 931-4723

Figure 2: Weak decays and the CKM matrix.

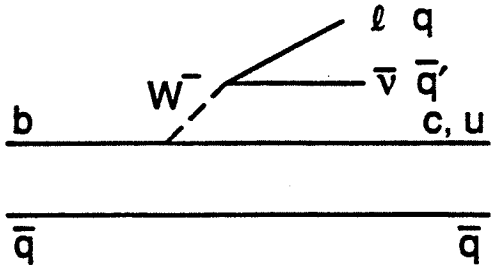

(a) Spectator, external

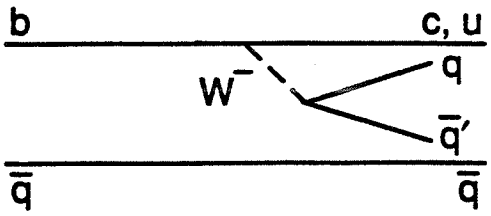

(b) Spectator, internal

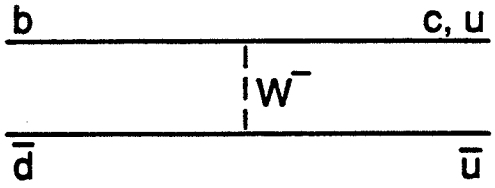

(c) Exchange

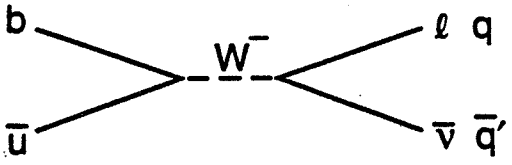

(d) Annihilation

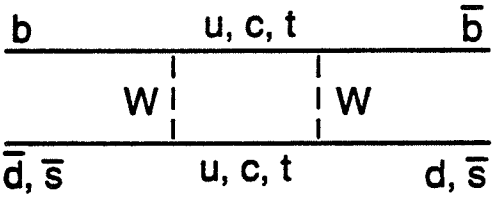

(e) Mixing

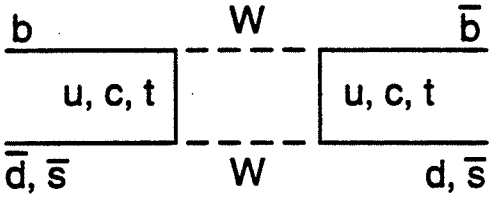

(e) Mixing

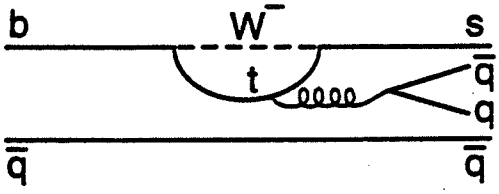

(f) Penguin

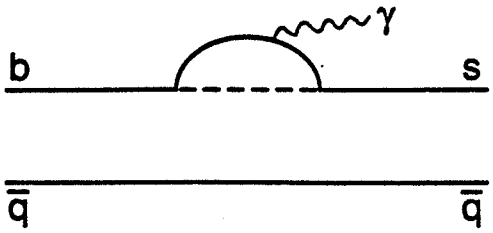

(g) E.M. Penguin

Figure 3: Feynman diagrams for B meson decays. XBL 932-4722

By studying the decays of B mesons we have access to a number of these matrix elements. In Fig. 3 the Feynman diagrams for a variety of B decays are shown. From spectator decays (Fig. 3a) we can measure V_{cb} and V_{ub}; the semi-leptonic decays, where the W decays to $\mu\nu$ or $e\nu$ are especially useful here since there can be no final state interactions between the W decay products and the other final state quarks. Internal spectator decays, shown in Fig. 3b, can occur only when the W decays to a pair of quarks. This diagram is color-suppressed relative to Fig. 3a, because only some combinations produce the allowed colorless final states.

There are also W exchange diagrams and annhilation diagrams, (Fig. 3c and 3d) both of which are expected to be small in the B system. The annhilation decay $B \rightarrow \tau\nu$ is especially interesting because it will provide direct information about the B decay constant, f_B. However the small branching fraction and the presence of neutrinos in the final state make it extremely difficult to detect. The mixing diagram (Fig. 3e) can give us information about V_{td} since the box diagram with the heaviest quark is dominant. In the case of mixing in the B_s system, we can obtain information about V_{ts}. Penguin diagrams (Fig. 3f and 3g) will allow us to measure V_{ts}. Penguins may also be a serious source of background to some CP violation studies, so it will be important to measure them in order to quantify this effect.

3 Where to B

In this section I will discuss the production of B mesons at several different types of accelerators and center-of-mass energies, and describe some of the experimental techniques which are employed in the study of B physics at each type of machine. We will cover e^+e^- machines operating at the $\Upsilon(4S)$, in the continuum, and at the Z^0, fixed target experiments, and hadron colliders.

3.1 B Physics On the $\Upsilon(4S)$

We begin with e^+e^- colliders running at a center of mass energy equal to the mass of the $\Upsilon(4S)$. Resonant production of the $\Upsilon(4S)$ is one of the best ways to produce B mesons because there is a relatively large resonant cross section of 1.2 nb sitting on a continuum background of 3.5 nb, for a very good signal to noise ratio of 1:3. In Fig. 4 the total hadronic cross section as measured by the CLEO experiment in the region around 10 GeV is shown; a total of four resonances are seen, corresponding to the four lowest radial excitations of the Υ. The $\Upsilon(4S)$ is noticeably broader than the other three, because it is just above the threshold to decay to a pair of B mesons.

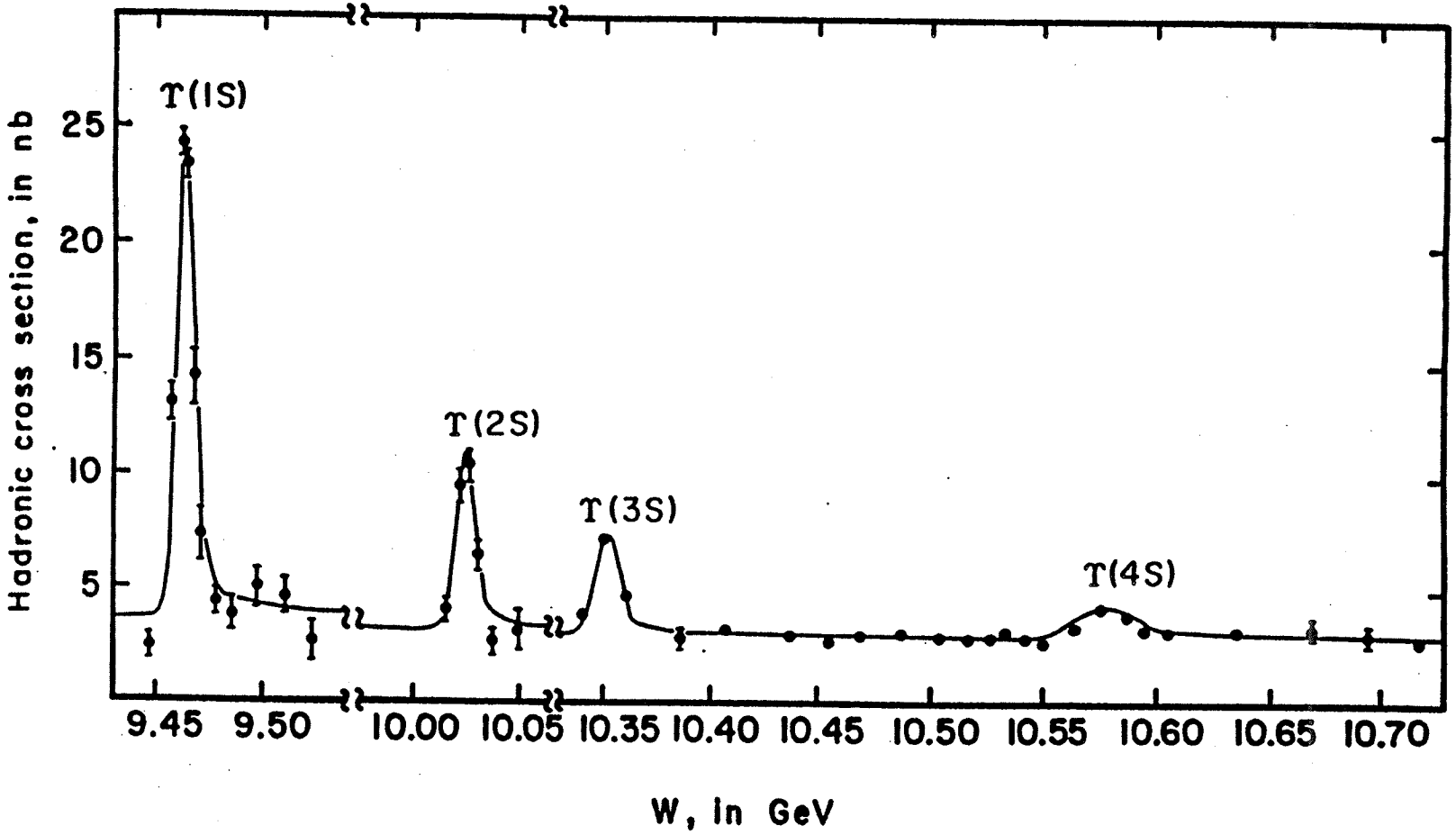

Figure 4: The cross section for $e^+e^- \rightarrow$ hadrons vs. c.m. energy, measured by the CLEO experiment.

In fact, the observed widths of the lower-lying states are dominated by the beam-energy spread which is about 2 MeV; their actual widths can be inferred by measuring the total cross section and the leptonic branching ratio. The intrinsic widths of these states are on the order of tens of keV, three orders of magnitude smaller than the width of the $\Upsilon(4S)$, which is about 24 MeV. If one assumes that the increased width of the $\Upsilon(4S)$ is due solely to the kinematic accessibility of the $B\bar{B}$ channel, then by taking the ratio of widths one would conclude that the $\Upsilon(4S)$ decays 99.9% of the time into $B\bar{B}$. Experimentally the limits are much less restrictive, and will be discussed in more detail below.

Because only B_d and B_u mesons can be produced on the $\Upsilon(4S)$, one does not have access to other states such as the B_s, B_c, or B baryons. However, B_d mesons are produced in a special quantum state on the $\Upsilon(4S)$, with $J^{PC} = 1^{--}$, and Bose statistics will cause them to evolve coherently until one decays. This has important ramifications for mixing and also for CP violation studies.

In addition to a large cross section and good signal-to-noise, there are other advantages in working at the $\Upsilon(4S)$. The mass of the $\Upsilon(4S)$ at 10.580 GeV was well-chosen by nature since it is just heavy enough to allow it to decay to a pair of B mesons, which have a combined mass of 10.557 GeV; there is not enough energy left over to produce any additional particles and therefore all of the particles in an event come from the decay of one of the two B's. There is a disadvantage to this as well, however: the B's are produced with a momentum of about 345 MeV, and travel only 30 μm on average before they decay, which is not far enough to be measured. Because they decay almost at rest, the decay products of the two mesons are produced isotropically; with an average of 5 charged particles and 5 photons per B decay the combinatorics of two overlapped decays can be very difficult to resolve.

There are several useful handles which can be used to separate $B\bar{B}$ events from the continuum background. For example, B's from the $\Upsilon(4S)$ are produced with a $\sin^2\theta$ dependence, where θ is the polar angle. This follows from helicity arguments and the fact that the B's are pseudoscalars produced in an L=1 state. The continuum process $e^+e^- \rightarrow q\bar{q}$ has a $(1+\cos^2\theta)$ dependence, so a simple fiducial cut requiring events to be centrally produced will enhance the signal to noise ratio.

Event topology can also be used to distinguish the two processes. Light quarks are produced with significant momentum and the $q\bar{q}$ pair will tend to hadronize as two jets of particles, whereas the heavier B's are produced almost at rest and their decay products are distributed isotropically. There are a number of event variables which are used to characterize event topology

and to separate jet-like events from isotropic events, such as the Fox-Wolfram moments [4], thrust [5], and sphericity [6]. Perhaps most important of all, there are some kinematic variables which uniquely characterize a $B\bar{B}$ event. Specifically, the momentum of the reconstructed B candidate must agree with the expected value of 345 MeV and the invariant mass must also be correct within the experimental resolution.

Finally, to estimate the remaining background after using all these kinematic and topological cuts, one can run slightly below the resonance in order to sample the continuum; after correcting for the slight difference in center-of-mass energy a subtraction is made to correct for any residual background. This is a very powerful tool, and is used extensively. In fact the total data sample collected off resonance is typically about half the size of the on-resonance data in experiments like CLEO and ARGUS.

In order to measure the properties of B_d and B_u mesons on the $\Upsilon(4S)$ we need two engineering numbers. The first one is the branching fraction for $\Upsilon(4S) \rightarrow B\bar{B}$, so that we can compute the total yield of B's correctly. As we discussed above, the naive assumption is that non-$B\bar{B}$ decays should account for only a fraction of a percent of all $\Upsilon(4S)$ decays. However it is possible that the $\Upsilon(4S)$ is not a pure $b\bar{b}$ state; or that some other decay processes are possible involving annihilation of the $B\bar{B}$ pair into another final state. (This mechanism been proposed as an explanation for non-$D\bar{D}$ decays of the ψ'' [7].)

Unfortunately, the experimental limits are not very stringent, because it is difficult to separate generic $B\bar{B}$ decays from non-$B\bar{B}$ decays of the $\Upsilon(4S)$. One way is to look for the production of particles with momenta beyond the kinematic limit for B decays; that is, assume a two-body B decay and compute the maximum momentum, taking into account the small boost of the B in the lab frame and the detector resolution. Anything beyond the kinematic endpoint cannot come from a B decay. Of course there will be particles beyond this endpoint produced in continuum $e^+e^- \rightarrow q\bar{q}$ events, but this contribution can be estimated and subtracted by running below the $\Upsilon(4S)$. CLEO has performed this analysis [8] using inclusive charged particles, and found an upper limit on non-$B\bar{B}$ decays of the $\Upsilon(4S)$ ranging from 3.8% (assuming a momentum spectrum like that from the continuum) to 13% (assuming a spectrum similar to that in $\Upsilon(1S) \rightarrow ggg$), both at 90% C.L..

In a similar type of analysis, both ARGUS and CLEO have searched for J/ψ's produced above the kinematic endpoint for production in B decays. Initially, both experiments reported a small excess of such events [9, 10], corresponding to a branching fraction for $\Upsilon(4S) \rightarrow J/\psi X$ of about 0.2%. This fueled a great deal of speculation about the source of such events. However,

in a more recent and much larger data set, CLEO has failed to confirm this result [11], and they have attributed their initial results to statistical fluctuations. So at present there is no experimental evidence for non-$B\bar{B}$ decays of the $\Upsilon(4S)$. We will generally assume that the $\Upsilon(4S)$ decays 100% into $B\bar{B}$, but it is good to keep in mind that this is not well-established.

The second engineering number that one needs in order to extract physics on the $\Upsilon(4S)$ is the ratio of charged to neutral B meson production, f_+/f_0. This, together with $\mathrm{Br}(\Upsilon(4S) \rightarrow B\bar{B})$, gives us the yield of $B^0\bar{B}^0$ and B^+B^- pairs, and is necessary for the determination of exclusive branching ratios of either charged or neutral B's, for $B^0\bar{B}^0$ mixing measurements, and so on. Unfortunately, it is also not experimentally well determined and we must rely on theoretical calculations. Because the $\Upsilon(4S)$ is very close to the threshold for production of $B\bar{B}$ pairs, this ratio is very sensitive to any difference in the B^+ and B^0 masses. Byers and Eichten [12] have calculated that if the B^0 is 2 MeV heavier than the B^+, f_+/f_0 would increase by 13%. As we will see later on, these masses are very close to being equal within the experimental uncertainty, but this uncertainty is on the order of 1 MeV.

There is an additional enhancement of B^+B^- production over $B^0\bar{B}^0$ production due to the Coulomb attraction, which increases the value of the wave function at the origin between the two charged mesons. Naively this could enhance B^+B^- production by as much as 18 % [14]. However, two recent theoretical calculations [12, 13] that take into account the finite size of the mesons have calculated the correction to be in the range of (-3 – +4) % or (5–7)%, respectively. These corrections are also a function of c.m energy as shown in Fig. 5, taken from ref. [12]. Taken together, the corrections due to meson masses and Coulomb effects could cancel out if the charged B were slightly heavier than the neutral B, or add if the situation were reversed. Thus the allowed theoretical range for f_+/f_0 is probably anywhere from 0.90 to 1.15. Clearly there is a need for some experimental input, but this will require a lot of data because one must exclusively (or at least semi-exclusively) reconstruct the B mesons to determine their charge.

The accelerators which operate at the $\Upsilon(4S)$ are DORIS and CESR, home to the ARGUS [16] and CLEOII [15] experiments, respectively. They are both collecting data now; ARGUS has a new vertex detector and the CLEOII detector is a major upgrade of the old CLEO which boasts a CsI calorimeter with very good energy resolution and a new vertex detector. The CESR storage ring has been substantially upgraded and has reached luminosities exceeding 2×10^{32} cm^{-2} s^{-1}.

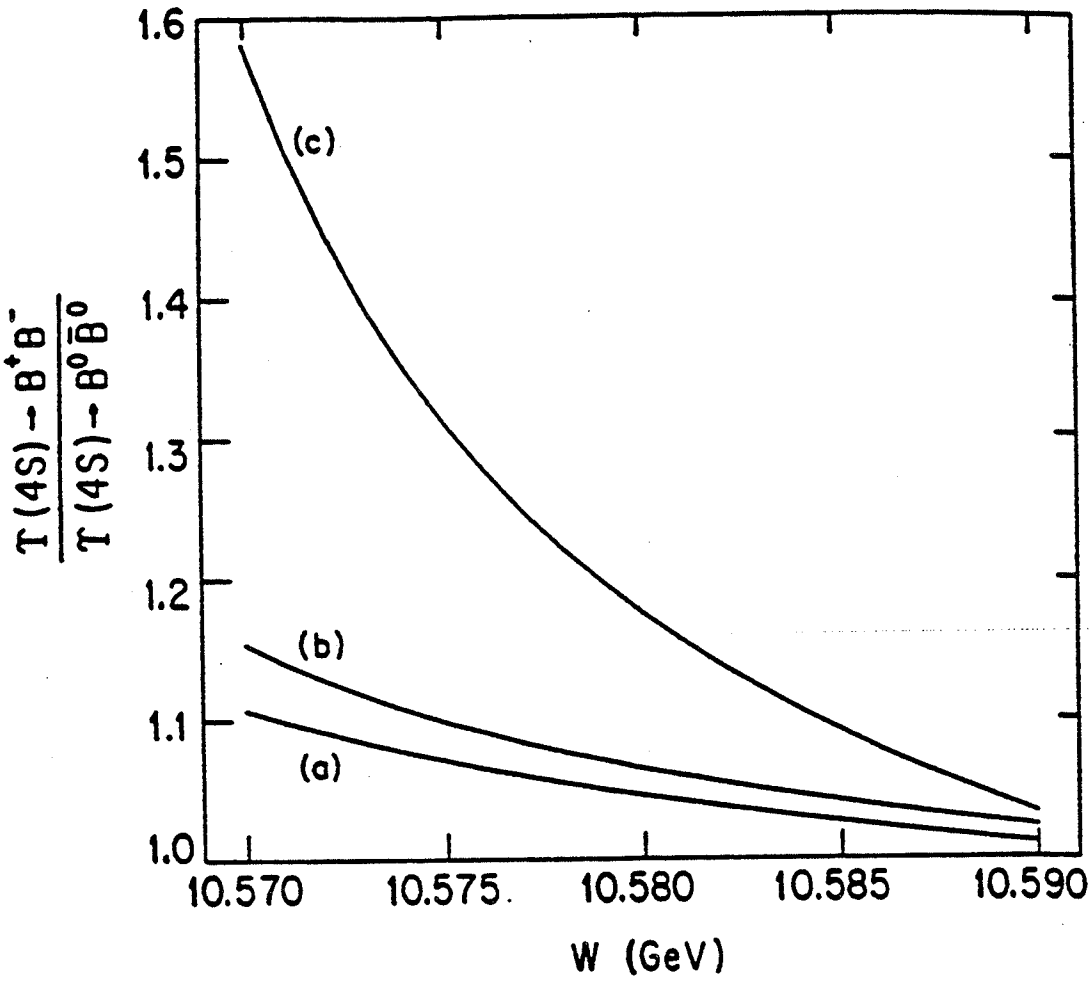

Figure 5: The ratio f_+/f_0 as a function of c.m. energy, for (a) $M_{B^+} = M_{B^0} = 5.278$ GeV, (b) $M_{B^+} = M_{B^0} = 5.280$ GeV, and (c) $M_{B^+} = 5.278$ GeV and $M_{B^0} = 5.280$ GeV, from ref. [12].

3.2 B Physics at e^+e^- Colliders in the Continuum

Moving up c.m. energy, we will next consider the production of $b\bar{b}$ pairs at e^+e^- colliders operating in the continuum, such as PEP, PETRA and TRISTAN. The b quarks hadronize independently as soon as we move off the $\Upsilon(4S)$ resonance, so that all possible combinations of B hadrons can be produced. In addition, other particles will generally be produced from the primary vertex, so each B hadron will carry only a fraction of the beam momentum. The relative rates for the production of the various flavors of B mesons and baryons has not been experimentally measured, but the usual assumption is that roughly 75% are B_d and B_u, 15% are B_s, and 10% are B baryons. (The production rate for B_c should be much smaller.) It is possible that these rates are a function of c.m. energy, and it is likely that excited states such as B^*'s are produced which decay strongly to the lower-lying mesons.

The total hadronic cross section falls as $1/s = 1/(4E^2_{beam})$. To calculate the cross section for $b\bar{b}$ we can just take the point cross section, 87 nb/s^2, multiply by a color factor of 3 and by the square of the quark charge. At PEP ($\sqrt{s} = 29$ GeV) the calculated cross section is $\sigma(e^+e^- \rightarrow b\bar{b}) = 35$ pb and at TRISTAN ($\sqrt{s} = 60$ GeV) the $b\bar{b}$ cross section is only 8 pb. These cross sections result in a rather small rate; furthermore, $b\bar{b}$ production is suppressed relative to $c\bar{c}$ production by the ratio of quark charges squared, a factor of 4. Thus charm constitutes a significant source of background. The total signal to noise ratio in hadronic events is 1:10.

Despite the lower production cross section and higher backgrounds, there is a significant advantage to operating in the continuum: the B's are moving in the lab frame and travel measurable distances before decaying. The average distance traveled is given by $\gamma\beta c\tau$, where $c\tau$ for B hadrons is about 400 μm. The factor $\gamma\beta$ is simply equal to p_B/m_b, and the B momentum will typically be about 70% of the beam energy. So at PEP and PETRA the B hadron travels almost a millimeter, on average, before decaying, making lifetime measurements quite feasible at these energies.

In addition to measuring the average B-hadron lifetime, experiments at e^+e^- colliders in the continuum have measured the forward-backward asymmetry in $b\bar{b}$ events (caused by interference between the virtual γ and Z^0 channels), the B-hadron fragmentation function and the average B-hadron semi-leptonic branching ratio.

Many important experimental techniques that are now being used by experiments operating at the Z^0 were pioneered in the earlier experiments at PEP and PETRA. One such technique is lepton tagging, in which an energetic lepton that has large momentum transverse to the event axis is

used to identify b decays. The event axis is usually defined either by the thrust or the sphericity axis; they are rather similar when applied to two jet events. The thrust axis $\hat{t}$ is defined as that which maximizes the thrust, T:

$$T = \frac{\sum \vec{p}_i \cdot \hat{t}}{\sum \vec{p}_i},$$

where the sum is over the momenta, $\vec{p}_i$, of all the particles in the event. The sphericity axis $\hat{s}$ is that which minimizes the sphericity S, defined by:

$$S = \frac{3\sum(\vec{p}_i \times \hat{s})^2}{2\sum \vec{p}_i^2}.$$

Leptons from a b quark decay will have a larger p_t relative to the event axis, on average, than leptons from the decay of a lighter quark such as charm, because the b quark is heavier and releases more energy in its decay. In addition to leptons from the desired process, $b \rightarrow l$, there are backgrounds from $c \rightarrow l$ decay, the cascade decay $b \rightarrow c \rightarrow l$, as well as muons from π and K decays in flight, and electrons from photon conversions. By requiring both a minimum total momentum (typically > 2 GeV at PEP or PETRA energies) and a minimum p_t (typically > 1.5 GeV), most of these background processes can be eliminated, resulting in event samples with about 60 % B's, 25 % charm and 15% other backgrounds.

In some analyses it is important to use the lepton tag to determine whether the decay was from a B meson (which by convention contains a $\bar{b}$ quark) or from a $\bar{B}$ meson (containing a b quark). A positive lepton tags a B decay while a negative lepton tags a $\bar{B}$ decay; however the background process $b \rightarrow c \rightarrow l$ always contributes a 'wrong-sign' tag. Other backgrounds such as conversions and decays in flight contribute a wrong-sign tag 50% of the time. The fraction of wrong-sign tags must be correctly estimated in an analysis such as $B\bar{B}$ mixing; it will also be important for future experiments doing CP violation measurements.

The disadvantage of using leptons to tag B's is that we have to pay the price of the leptonic branching ratio, which is about 11% for each lepton species. In order to increase the efficiency for certain types of analyses which do not require a lepton, one can use an event shape variable called the boosted sphericity product. In this technique one first finds the event axis, then divides the event into two hemispheres each containing one of the jets. By boosting each half independently into its rest frame, assuming the mass of the b quark, one should obtain an isotropic distribution of particles which exhibits a large sphericity. The product of the two sphericity variables is called the boosted sphericity product, and it will be larger for $b\bar{b}$ events than for light quark events. The purity is lower than that obtained for a high p_t

lepton tag but the efficiency is higher. Recently this technique has been used at the Z^0 by the DELPHI experiment in order to measure the partial width for $Z^0 \rightarrow b\bar{b}$ [17]; they achieved an efficiency of about 30% but the purity was low, also about 30%.

At present the only e^+e^- accelerator running in the continuum above $b\bar{b}$ threshold is TRISTAN. All three detectors at TRISTAN have recently been upgraded with the addition of vertex detectors, and there are plans to measure the forward-backward asymmetry in $b\bar{b}$ events, taking advantage of the large $\gamma - Z^0$ interference term at the TRISTAN energy of 60 GeV.

3.3 B Physics on the Z^0

B physics on the Z^0 resonance is an interesting combination of the features just described above for the $\Upsilon(4S)$ and the e^+e^- continuum. The standard model defines the couplings of the Z to fermion–anti-fermion pairs in terms of a few fundamental constants:

$$\Gamma(Z^0 \rightarrow f\bar{f}) = \frac{G_F M_Z^3}{6\sqrt{2}\pi}(g_V^2 + g_A^2),$$

where G_F is the Fermi constant and M_Z is the Z^0 mass. In the table below, g_V and g_A, the axial and vector coupling constants, are given for each type of fermion and the resulting Z^0 partial width is calculated. From this table we note that the Z^0 couples more readily to down-type quarks than to up-type quarks or to leptons.

Fermion	g_V	g_A	$\Gamma(Z^0 \rightarrow f\bar{f})$(MeV)
ν	1/2	1/2	166
l	$-1/2 + 2\sin^2\theta_W$	$-1/2$	83.5
u	$-1/2 - 4/3\sin^2\theta_W$	1/2	285
d	$-1/2 + 2/3\sin^2\theta_W$	$-1/2$	369

Table 1: Z couplings and partial widths in the Standard Model

The partial width of $Z^0 \rightarrow b\bar{b}$ has been experimentally measured at both LEP and SLC, and the average value quoted by the Particle Data Group (PDG) [18] is 378.4 ± 26 MeV, in good agreement with the Standard Model

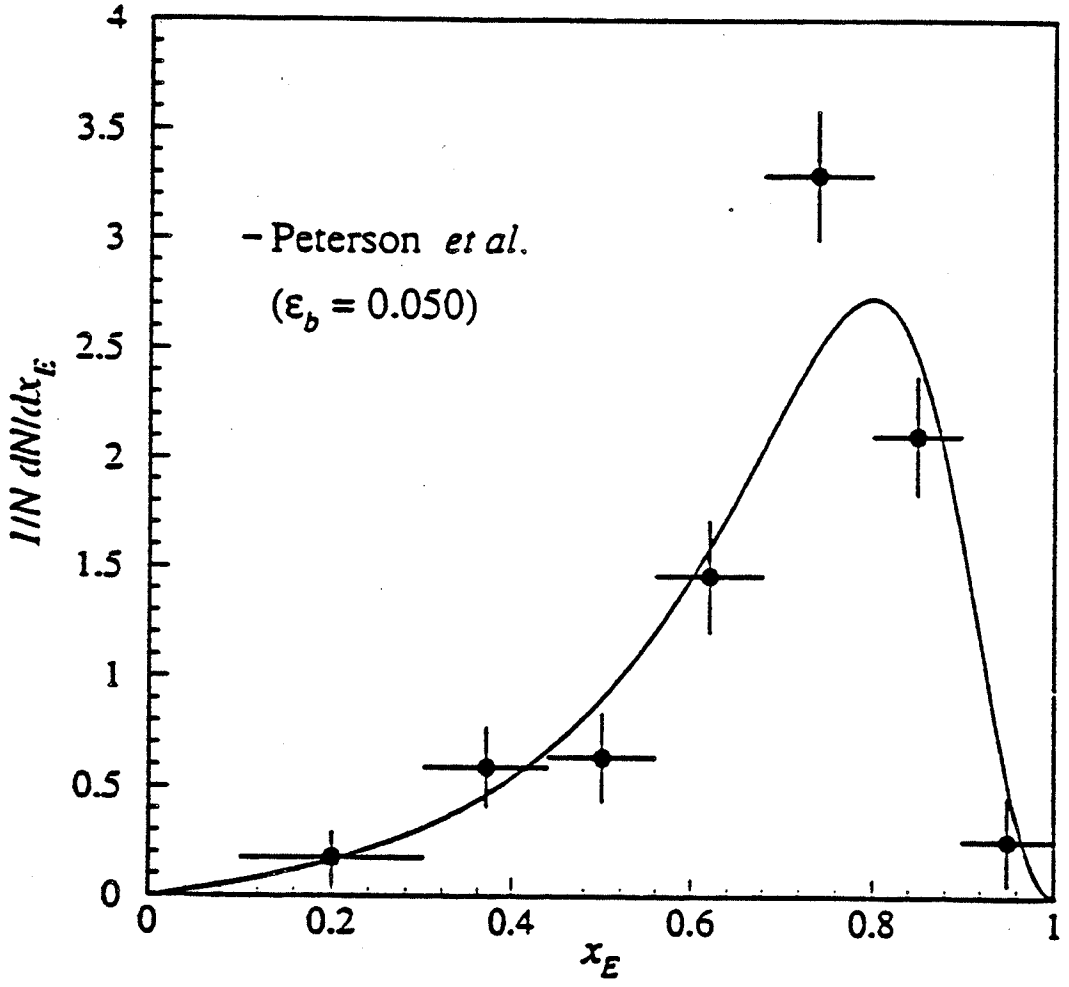

Figure 6: The measured b-quark fragmentation function $f(X_E)$, fit with a Peterson function, from L3 (ref. [20]).

prediction The resonant cross section on the Z^0 is large, resulting in a total production cross section for $Z^0 \to b\bar{b}$ of about 4.6 nb and a signal-to-noise ratio in hadronic events of 1:4. This is a larger production cross section than on the $\Upsilon(4S)$ and the signal-to-noise ratio is almost as good; in addition one has the advantages of moving B's ($\gamma\beta c\tau \approx 2$ mm) and access to the B_s and Λ_b states.

However, just as in continuum e^+e^- production, the b quarks hadronize independently and the momentum of the B hadron depends on quark fragmentation. The fraction of the beam energy carried off by a B hadron, denoted X_E, has been experimentally determined by fitting the Peterson fragmentation function [19] to the measured lepton momentum and p_t spectra. The X_E distribution and fit to the data from L3 [20] are shown in Fig. 6; they find a mean value of $X_E = 0.686 \pm 0.006 \pm 0.016$. From the distribution it is clear that there is a fairly wide spread in the momenta with which B hadrons are produced. The kinematic and topological handles available on the $\Upsilon(4S)$ to reject background are not available on the Z^0, and once again one must use high p_t leptons, the boosted sphericity product, or look for separated vertices to tag B's. Running off resonance to estimate the background contribution will not work either, because most of the background is due to Z^0 decays to other final states. Instead one must rely on Monte Carlo for most background estimates.

There is an important advantage which one has if longitudinally polarized electrons are collided to produce Z^0's: the large forward-backward asymmetry in $z^0 \to b\bar{b}$ can be used to tag the sign of the B hadron [21]. The SLC has succeeded in producing polarized Z^0's this summer, so this feature may be utilized in the future by the SLD experiment.

The LEP experiments have acquired very large data samples by now, on the order of 450,000 Z^0's each in 1991 and the hope is to log twice that in the present run. Three of the four experiments have installed silicon vertex detectors, and we can expect a great improvement in several areas of B physics in the near future. The results from these detectors include the partial width, lifetimes, both average and flavor-tagged, $B\bar{B}$ mixing, the forward backward asymmetry in $b\bar{b}$ events, and searches for other flavors such as the B_s and the Λ_b. Preliminary evidence for these states has already been found; this will be discussed in more detail below.

3.4 B Physics at Fixed Target Experiments

In any general lecture on B physics, the discovery of the Υ in a fixed target experiment at FNAL in 1977 by Leon Lederman and co-workers must be mentioned. In fact, Lederman *et. al.* discovered two resonances: in 1976

they saw an enhancement in the e^+e^- invariant mass spectrum at about 6 GeV/c^2 [22], which later came to be known as the Oops-Leon. However in the next experiment, performed just a year later, they did discover a real resonance, this time in the $\mu^+\mu^-$ invariant mass spectrum [23]. The steeply falling invariant mass spectrum is shown in Fig. 7, together with the background-substracted spectrum. A broad peak is obvious in both plots; in fact the peak was broader than the intrinsic resolution of the experimental apparatus, giving an indication of more than one resonance. We now know that this was due to the radial excitations of the $\Upsilon(1S)$.

Since 1977 the forefront of B physics has moved to other types of accelerators, and the subject of B-physics at fixed-target experiments has received relatively little mention. However in recent years, with the increased interest in B physics there has also been renewed interest in the feasibility of doing B-physics in the fixed-target environment, and a number of experiments have been proposed and carried out. In the fixed target mode, the center of mass energy only grows as the square root of the beam energy, so using the highest available energy extracted proton beam, which is 800 GeV at the Fermilab Tevatron, one can only reach 39 GeV in the center of mass. On the other hand, very high luminosities can be achieved. The luminosity for fixed target experiments is calculated as the product of the number of particles per second in the incident beam and the density of particles in the target; assuming a beam intensity of $10^{10}s^{-1}$ and a typical target density of 10^{24} cm^{-2} one obtains a luminosity of 10^{34} cm^{-2}s^{-1}. However it should be noted than many fixed-target experiments cannot tolerate such a high rate.

The cross section for hadro-production of B's is about 10 nb using an 800 GeV proton beam. For a given beam energy, the $b\bar{b}$ cross section is higher for a π beam than for a proton beam. This is due to the contribution of the process $q\bar{q} \rightarrow b\bar{b}$, which is highly suppressed in pN interactions but not in πN interactions. In Fig. 8 the theoretical prediction by Nason, Dawson and Ellis [24], as evaluated by Berger [25] for $\pi + N \rightarrow b\bar{b}x$, is shown together with one experimental data point from WA78 [26]. The fixed-target production cross sections for $b\bar{b}$ are large compared those in e^+e^- collisions, but rather modest relative to a hadron collider, where the center of mass energy is so much greater. The primary disadvantage in fixed-target experiments is the very poor signal-to-noise ratio of about 3 x 10^{-7}. Photo-production is expected to yield a signal to noise ratio which is a factor of 20 better; however the absolute cross section for photo-production of beauty is very small, only about 0.5 nb for a 200 GeV photon beam, as illustrated in Fig. 9 (taken from ref. [32]). By contrast the photo-production cross section for charm is about 1 μb. Some very nice charm physics has been done using photo-production, but with such a low cross section it will be hard to duplicate that achievement

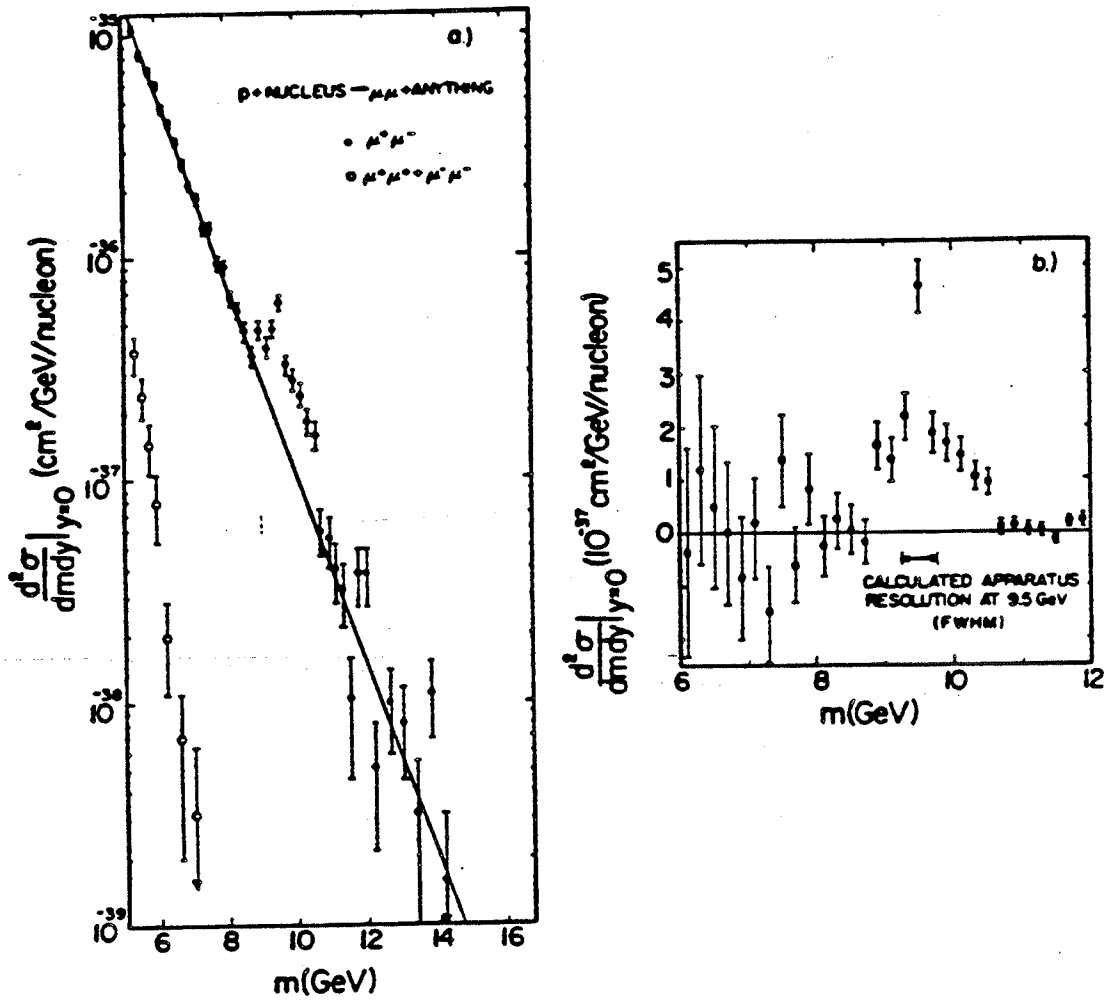

Figure 7: The discovery of the Υ: invariant mass of $\mu^+\mu^-$ pairs, from. ref. [23].

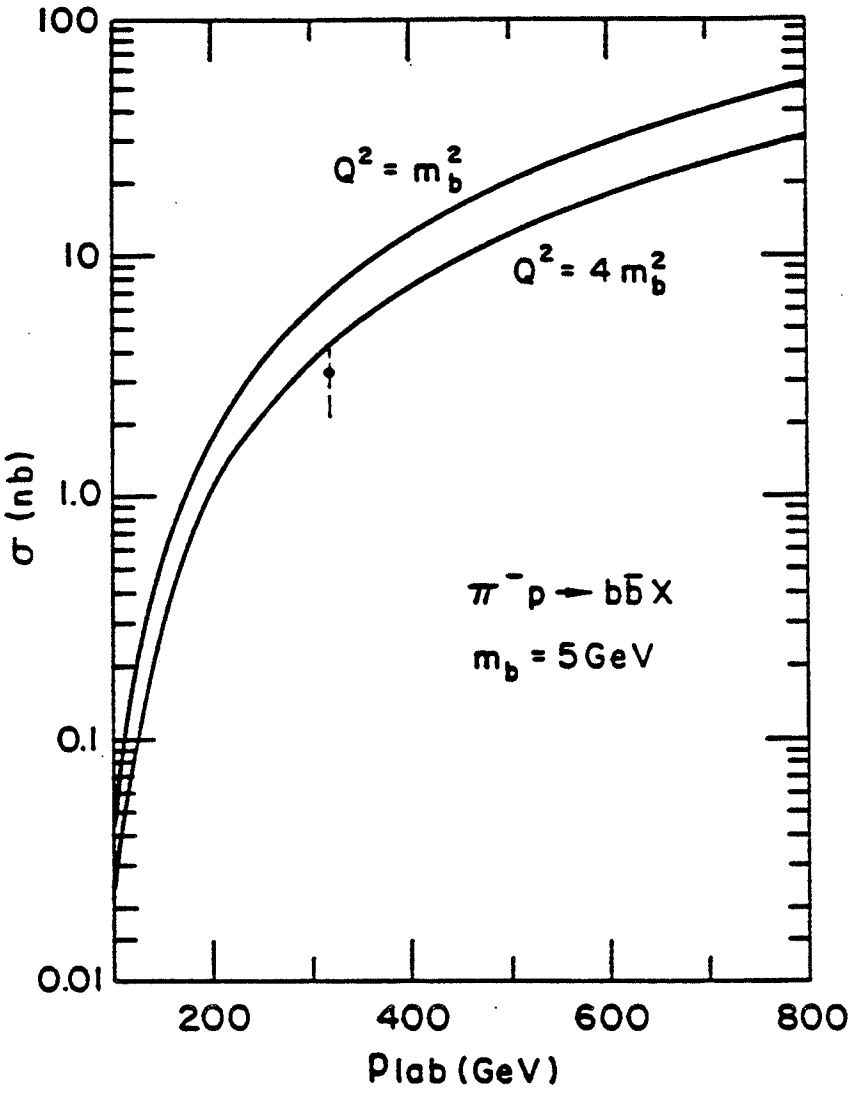

Figure 8: Cross section for the hadroproduction of beauty, taken from ref. [25].

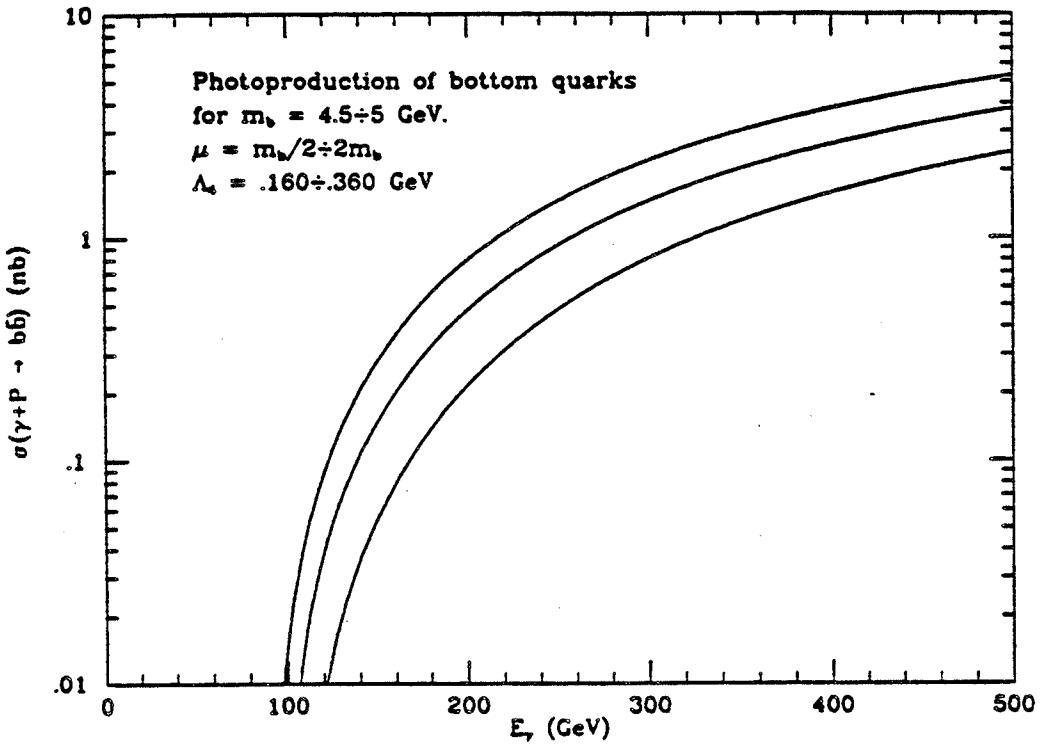

Figure 9: Cross section for the photoproduction of beauty, from ref. [32]. The bands represent an estimate of the theoretical uncertainty.

for B physics.

Fixed target experiments in B physics have taken several different approaches. One approach is to have an open geometry with a very large acceptance and just write everything to tape. Some examples of this approach are WA84 [27] at CERN, and E687 [28] and E791 at Fermilab. E791, for example, just finished a big run in which they collected 20 billion events; this represents a significant computational load. However, the $b\bar{b}$ yield assuming an unbiased trigger is only $2 \cdot 10^{10} \times 3 \cdot 10^{-7} = 6000$ events, and most of them will be difficult to distinguish from the background. For this reason E791 is primarly a charm experiment, and it will be a real coup if they succeed in reconstrucing even a handful of B's in any given final state.

A second approach is to have a more selective trigger, requiring two or more muons, or one muon with significant p_t. A di-muon trigger is useful because it accepts $B \rightarrow J/\psi X$ events, which constitute about 1% of all B decays. The displaced J/ψ vertex can be found offline, and its position gives the decay point of the B, allowing a lifetime to be extracted. Both WA78 [26] and NA10 [29] at CERN have taken this approach and used events with 2 or 3 muons in them to determine the hadro-production cross section; their results are in good agreement with the theoretical prediction. The E653 collaboration at FNAL has used a combination of nuclear emulsion and silicon vertex detectors to measure the flight path for $B \rightarrow \mu X$ events [30]. They have reported a result for the ratio of the B^+ and B^0 lifetimes in which the charged lifetime is longer than the neutral lifetime: $\tau_+/\tau_0 = 4.74^{+3.61+0.99}_{-2.60-0.51}$. However, the result is based on 18 B candidates, only 6 of which are charged. (The neutral B lifetime they report is consistent with the world average while the charged B lifetime is 2σ larger.) E771 is another fixed-target experiment with a muon trigger at Fermilab; it is presently running and expects to detect about 20 $B \rightarrow J/\psi X$ events and about 500 $B \rightarrow \mu X$ events.

A third approach is to use a very restrictive trigger to search for rare decay modes of B's. E789 has adopted this tactic in the search for di-hadron decays such as $B \rightarrow \pi^+\pi^-$ and $B \rightarrow \pi^- K^+$. They will also place limits on $B \rightarrow e^+e^-$ and $B \rightarrow \mu^+\mu^-$. The E789 apparatus consists of a double arm spectrometer with a very small acceptance, but to compensate they plan to take the maximum rate of $\approx 10^{10}$ incident particles per second and to use their silicon vertex detector in the trigger in order to maximize the $b\bar{b}$ yield. In the present run they hope to accumulate a few dozen $B \rightarrow J\psi X$ events and to set a limit on $B \rightarrow \pi^+\pi^-$ at the 10^{-4} level.

3.5 B Physics at Hadron Colliders

Until rather recently, the idea of doing B physics at a hadron collider would have been met with great skepticism. However the results in the past few years from the UA1 experiment at CERN and the CDF experiment at Fermilab have caused skepticism to give way to optimism, and there is presently a great deal of effort going on in this area. The primary motivation for doing B physics at a hadron collider is that the $b\bar{b}$ cross section at typical collider energies is enormous. For example at $\sqrt{s} = 1.8$ TeV it is about 50μb, with a signal-to-noise ratio of about 1:1000. At a hadron collider the b quarks hadronize independently, and all possible beauty mesons and baryons can in principle be produced; and the B's are often produced with large boosts. The production fractions are generally assumed to be similar to those in the e^+e^- continuum or at the Z^0, as previously discussed.

There are several processes that contribute to $b\bar{b}$ production at a hadron collider. There are the so-called $2 \rightarrow 2$ processes: $q\bar{q} \rightarrow b\bar{b}$ or $g\bar{g} \rightarrow b\bar{b}$, and there are higher order $2 \rightarrow 3$ processes involving gluon splitting and flavor excitation. To obtain the cross section for heavy quark production, the cross section for the most important hard-scattering processes must be computed and then convoluted with the parton density functions for the proton and anti-proton constituents. The α_s^3 QCD calculation of the short-distance, hard scattering cross section by Nason, Dawson and Ellis [31] showed that the higher order processes are important, being larger than the lower order processes for $p_{t,b} > 10$ GeV/c or so. This is illustrated in Fig. 10, which shows the total integrated cross section for $p_{t,b} > p_{t,min}$, as well as the $2 \rightarrow 2$, gluon splitting, and flavor excitation contributions [33]. The total cross section peaks at low values of b quark transverse momentum, and the rapidity distribution is very broad with an enhancement in the forward and backward directions; see Fig. 11, taken from ref. [34]. Requiring a minimum b quark p_t causes the cross section to be even more forward-peaked. This behavior creates a problem for collider detectors, which up until now have been primarily designed for centrally-produced, high p_t processes. It is also a challenge to identify and trigger on $b\bar{b}$ events, which look very much like other low-energy QCD processes, without completely swamping the available trigger bandwidth.

To enhance the B signal at a hadron collider the usual approach is to look for high p_t leptons. Leptons are fairly rare in the collider environment, where QCD processes dominate and mainly hadrons are produced. A lepton is often a signal of the weak interaction process; in fact, CDF has estimated that 90% of all electrons with $p_t > 12$ GeV/c come from B's, once electrons from W and Z boson production have been subtracted. The p_t spectrum for

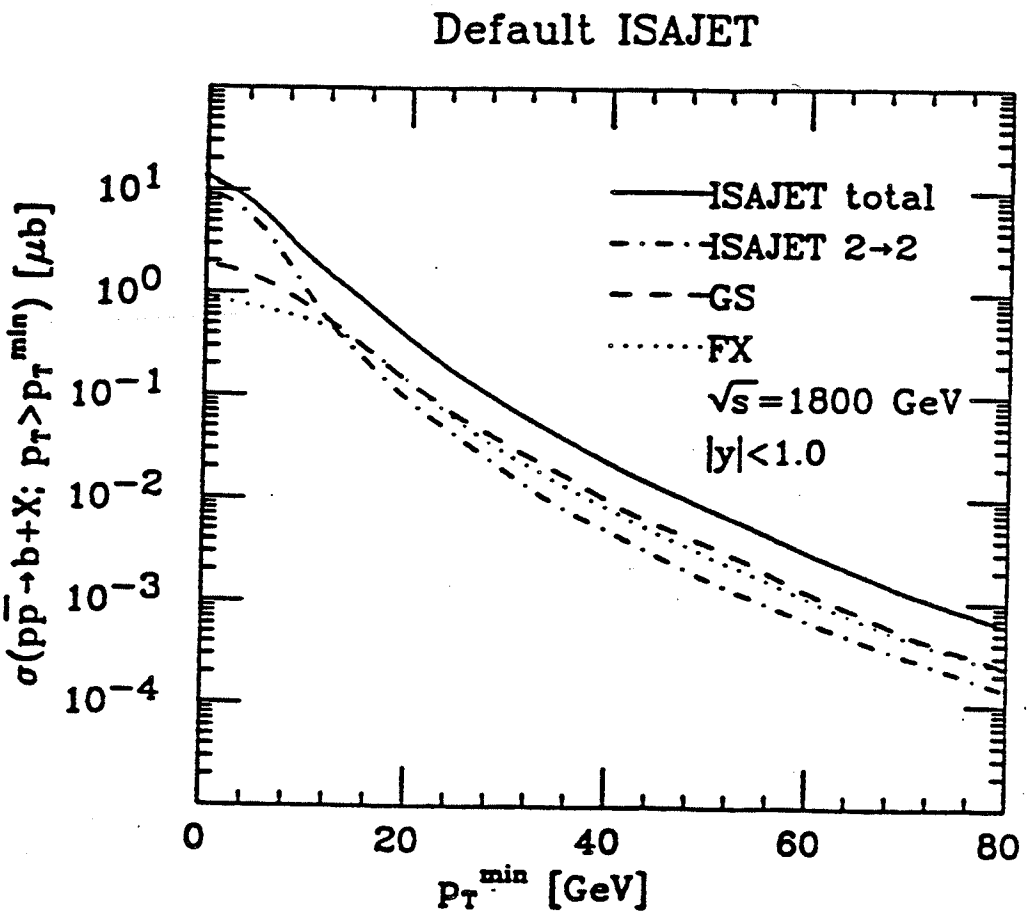

Figure 10: The production cross section for $p\bar{p} \rightarrow b + X$ from an Isajet calculation showing the lowest order $2 \rightarrow 2$, gluon-splitting (GS) and flavor excitation (FX) contributions, for $p_{t,b} > p_{t,min}$ and $|y| < 1$, from ref. [33].

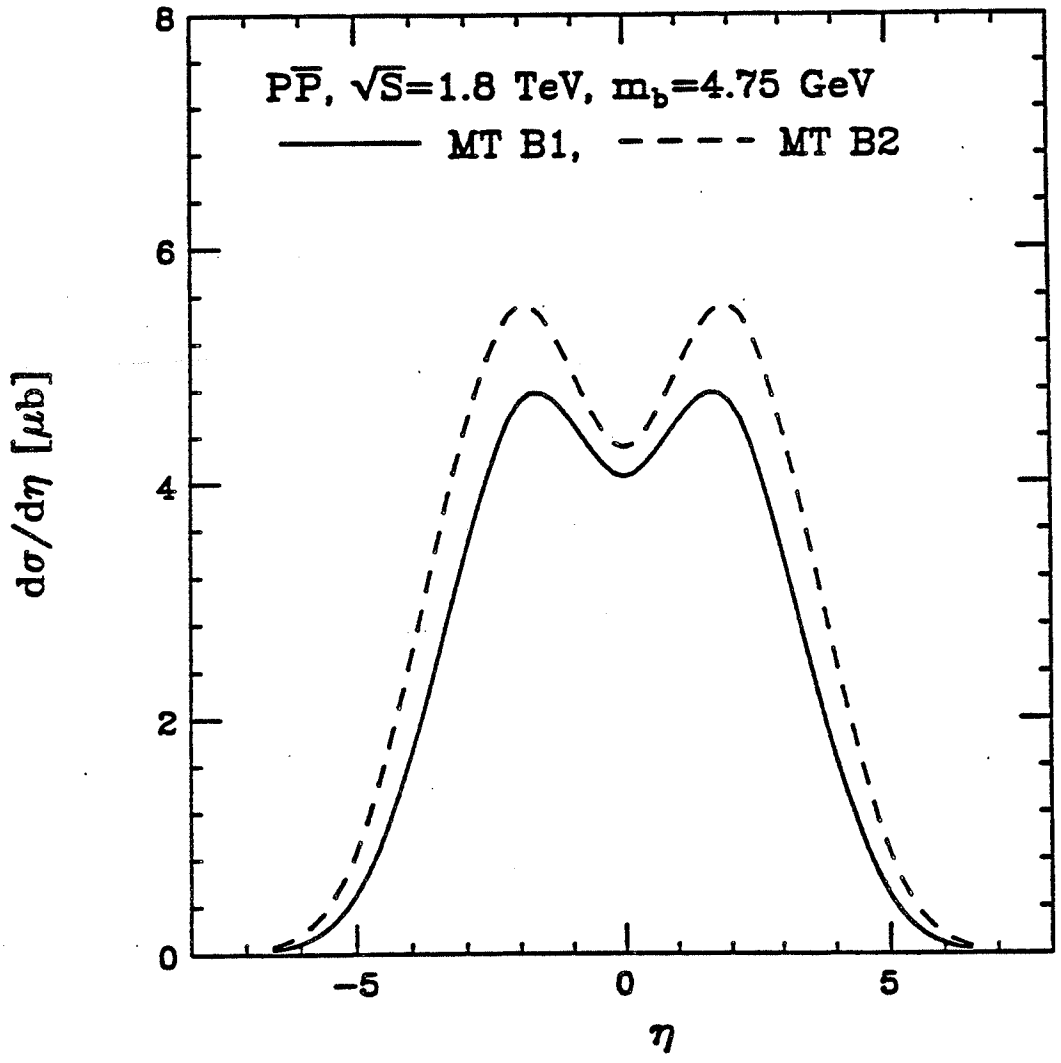

Figure 11: The rapidity distribution of b quarks produced in $p\bar{p}$ collisions at a center of mass energy of 1.8 TeV, from ref. [34].

electrons from CDF is shown in Fig. 12, taken from ref. [37], with the spectra for electrons from beauty and charm superimposed; the electrons from weak boson decay have now become a 'background' to the beauty signal. Another advantage of using high p_t leptons to identify B's is that they are easy to trigger on; in fact, all of CDF's B samples are from either electron or muon triggers. The acceptance for B's will increase greatly if the p_t threshold can be reduced, and the rapidity coverage extended, and CDF is attempting to improve on both fronts. In their 1989 data CDF had a threshold of 12 GeV for electrons, but they hope to lower this to about 9 GeV in the present run. They are also extending their muon coverage from $|\eta| < 0.6$ out to $|\eta| < 1.0$.

Another useful signature for B's at a hadron collider is the decay $B \rightarrow J/\psi + X$, with $J/\psi \rightarrow e^+e^-$ or $\mu^+\mu^-$. The inclusive branching fraction for $B \rightarrow J/\psi + X$ is about 1%, and the leptonic branching fraction of the J/ψ is about 6%. So the product branching fraction is only 1.2×10^{-3}, but with such a large production cross section one still finds an appreciable signal. It is also possible to trigger on a di-lepton event with lower trigger thresholds than for single leptons. In Fig. 13 the production cross section for J/ψ's at the Tevatron is shown, from a calculation by Glover, Martin and Sterling [38]. The process $B \rightarrow J/\psi + X$ dominates at high p_t and central values of rapidity. However, at lower p_t and higher rapidity, the process $\chi \rightarrow J/\psi + \gamma$ begins to dominate. This presents a challenge: as one pushes to lower p_t and higher rapidity in order to increase the acceptance for $b\bar{b}$, the background from charmonium production increases, reducing the signal-to-noise ratio.

The UA1 experiment has measured the inclusive production of J/ψ's [39] and estimated the fraction which are due to B's by studying the J/ψ isolation. J/ψ's from B's should be accompanied by some jet activity and will not be isolated, while those from the process $\chi \rightarrow J/\psi + \gamma$ will be isolated. They estimate that for $p_t > 5$ GeV/c and $|\eta| < 2$, 69% of the J/ψ's are due to charmonium production and 31% come from B's. This result agrees with the total production cross section for B's which UA1 has independently measured using high-mass di-muons [40].

Another signal for B production which is, in principle, even better than J/ψ's is ψ''s. The inclusive branching ratio for $B \rightarrow \psi' X$ is about half of the inclusive branching ratio to J/ψ's, but the background contributions are expected to be an order of magnitude lower, so that to first order all ψ''s come from B's. Unfortunately the leptonic branching ratio of the ψ' is also lower than that of the J/ψ by an order of magnitude, and it is more difficult to reconstruct in its more copious decay modes, like $J/\psi\pi^+\pi^-$.

The CDF experiment has observed a large J/ψ signal, and they have succeeded in combining the J/ψ with a K^+ to obtain a signal of about 14.1 ± 4.3 events at the B^+ meson mass; see Fig. 14, from ref. [41]. (Because CDF

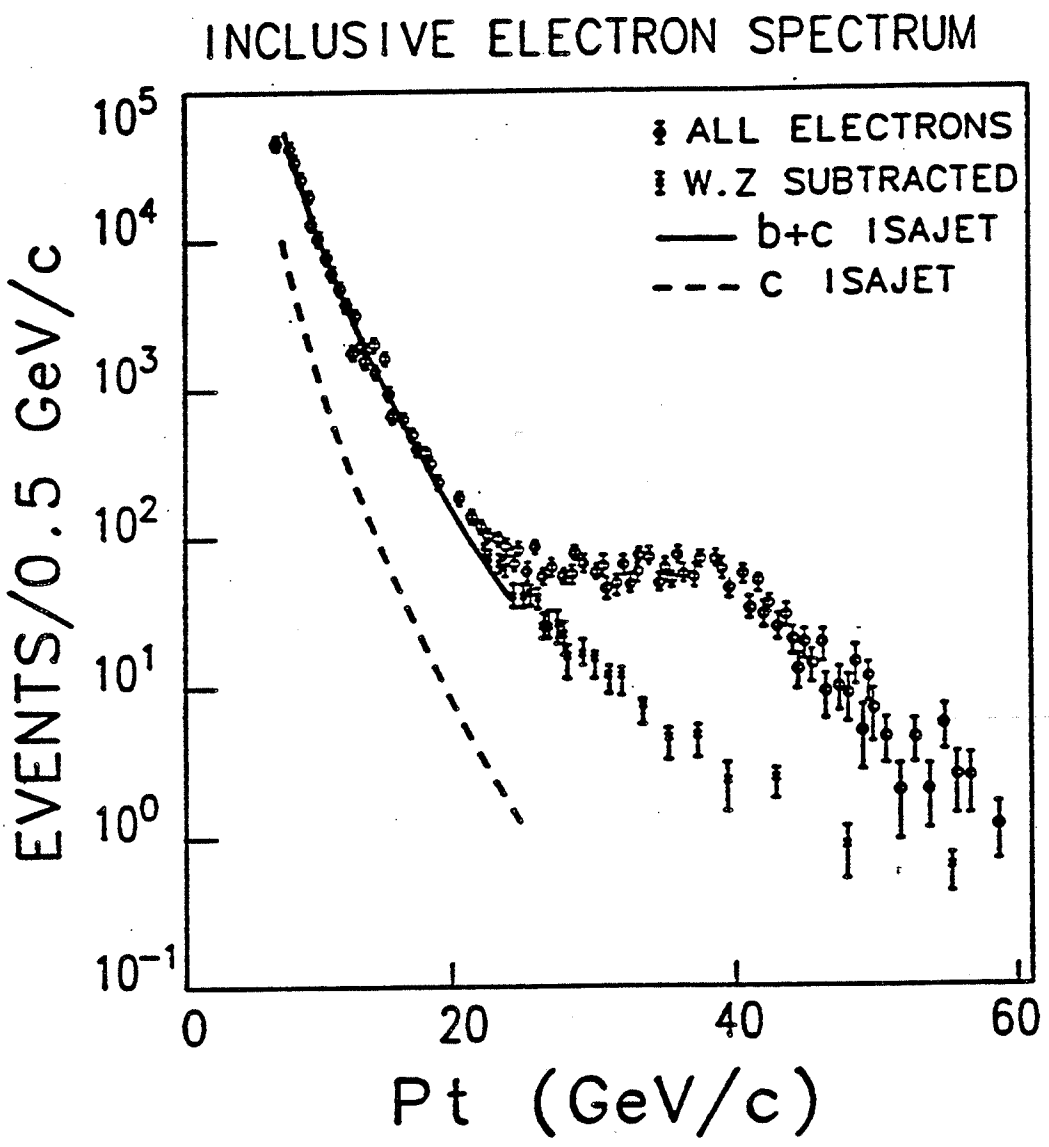

Figure 12: The electron p_t spectrum observed by CDF, from ref. [37]; the data are for all electrons, and for all electrons with W and Z substracted. The fit is to an Isajet prediction with relative normalization.

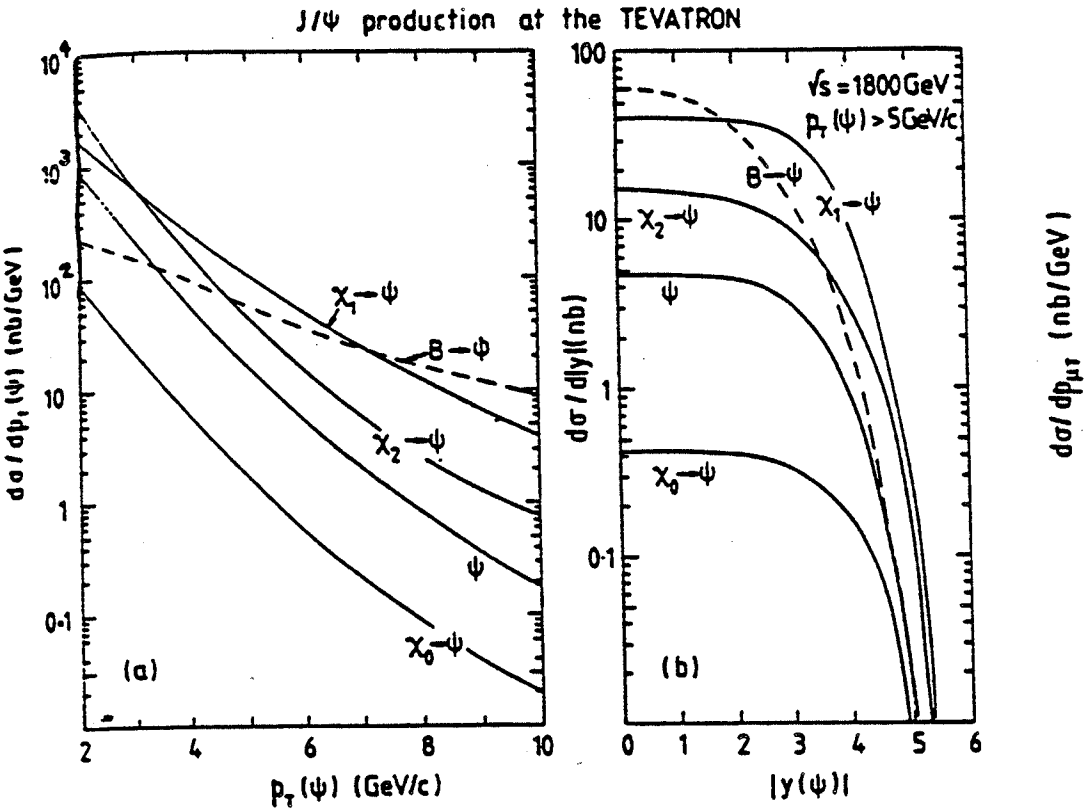

Figure 13: Sources of J/ψ production at the Tevatron collider, from ref. [38].

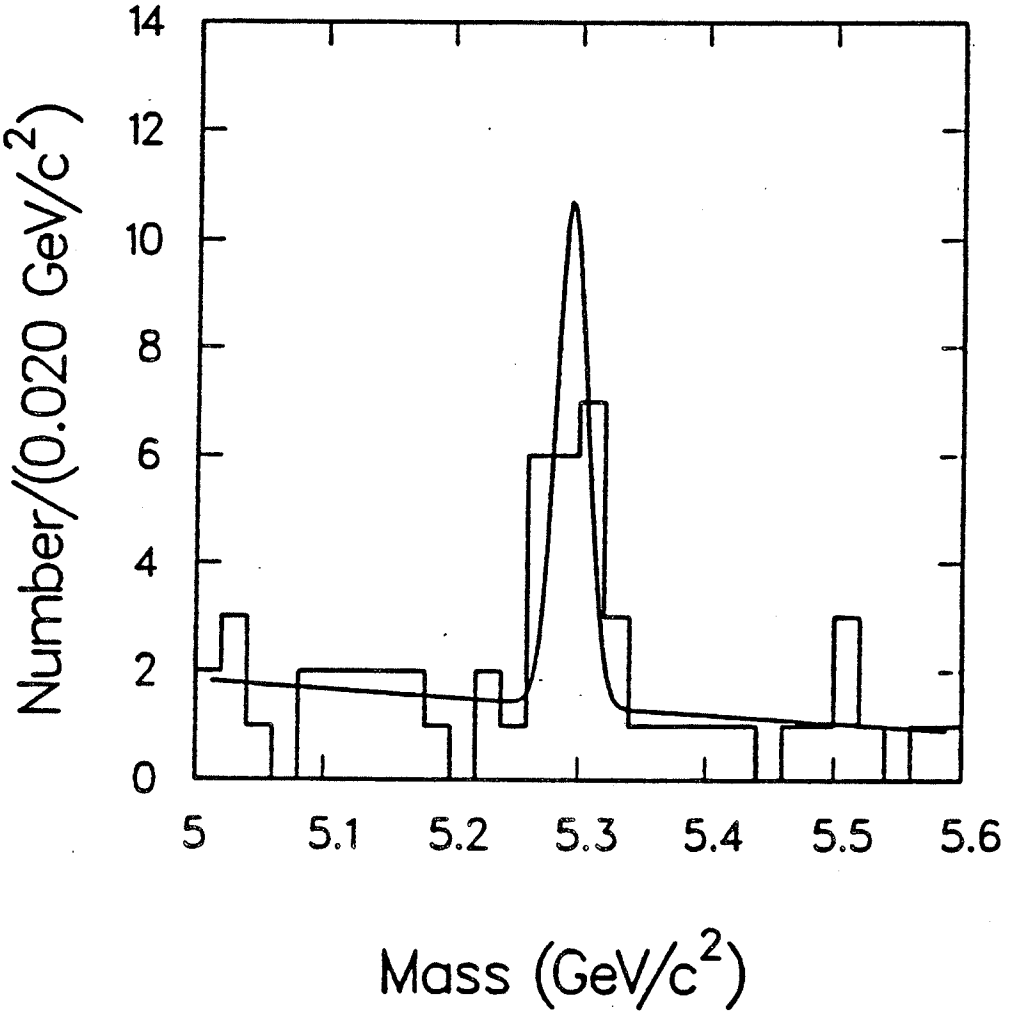

Figure 14: The invariant mass distribution from CDF for $\mu^+\mu^-K^+$ events, from ref. [41].

has no particle ID, the 'K^+' is simply a charged particle which is assumed to have the mass of the K^+.) The raw yield of events in the channel $B \rightarrow J/\psi K^+ \rightarrow \mu^+\mu^- K^+$ was over 6000 for their data sample of 2.6 pb^{-1}, so the efficiency to trigger and reconstruct these events was only about 0.25%. This illustrates the difficulty involved in reconstructing even a clean final state at a hadron collider. Much of the loss of efficiency is due to trigger thresholds and geometric acceptance, both of which have been improved in CDF for the present run, as previously mentioned.

Both CDF and UA1 have measured the total production of B's using a variety of techniques, including single electrons and muons, high mass dimuons, and J/ψ's. The results have been combined into a single plot, see Fig. 15, taken from ref. [36]. The UA1 data, at $\sqrt{s} = 630$ GeV, agree fairly well with the α_s^3 QCD prediction, while the CDF data, at $\sqrt{s} = 1.8$ TeV, are systematically higher than the prediction. The gluon-gluon subprocess is more important at the higher energy, and involves a lower average value of $x = 2M_t/\sqrt{s}$, where $M_t^2 = p_t^2 + m_q^2$, and p_t and m_q are the transverse momentum and mass of the produced heavy quark. It has therefore been suggested that perhaps the discrepancy can be fixed by modifying the gluon density function at low x [36]. It is also possible that α_s^4 processes are non-negligible at the Tevatron energy.

In any case more data will soon be available to sort out this puzzle. The Tevatron is presently running with two detectors, CDF and D0, and is expected to deliver 100 pb^{-1} in the next two years, which is factor of 20 over previous data samples. Both experiments will study the $b\bar{b}$ production properties and the greatly improved statistics should help to clarify this situation. In addition, CDF has recently installed a silicon vertex detector; this should help in tagging B's and allow them to improve their signal-to-noise for exclusive final states. The D0 detector is non-magnetic, but has a very large muon system extending to low angles with a magnetized iron toroid, so that charge and momentum measurements are available for muons. This capability will be exploited in order to make measurements of the $b\bar{b}$ production cross section over a large solid angle.

3.6 Summary of Where to B

In Table 2 the center of mass energy, luminosity and production cross section for $b\bar{b}$ production and $b\bar{b}$ yield per year are summarized for the e^+e^- and $p\bar{p}$ accelerators which are still operating. Some of the advantages and disadvantages of each are summarized in the last column. In rate it is clear that the Tevatron collider wins hands down; also, the B's at the collider are boosted and all flavors are produced. However, it suffers from a very

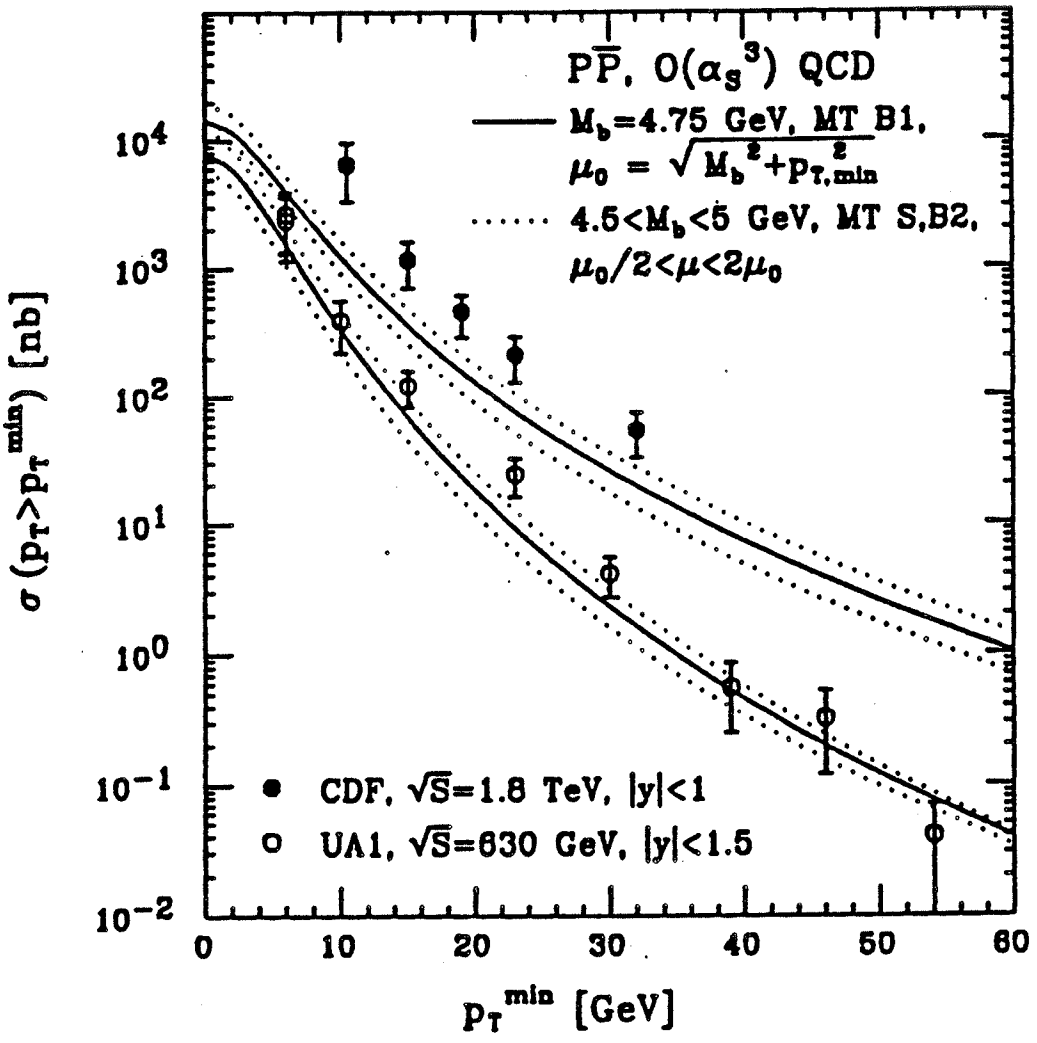

Figure 15: The integral cross section for $p\bar{p} \rightarrow b + X$, for $p_{t,b} > p_{t,min}$. The data from CDF and UA1 are shown together with the theoretical prediction as calculated by Berger and Meng in ref. [36].

Machine	$\sqrt{s}$	$L, cm^{-2}s^{-1}$	$\sigma_{b\bar{b}}$	$\sigma_{b\bar{b}}/\sigma_{had}$	$N_{b\bar{b}}/10^7 s$	Comment
DORIS	10 GeV	2×10^{31}	1.2 nb	1/ 4	1.6×10^5	+ $\Upsilon \rightarrow B\bar{B}$ - Rate; At rest; Bd, Bu only
CLEOII	10 GeV	2×10^{32}	1.2 nb	1/ 4	1.6×10^6	+ $\Upsilon \rightarrow B\bar{B}$ - At rest; Bd, Bu only
TRISTAN	60 GeV	1×10^{31}	0.008 nb	1/11	800	+ All flavors; Lifetimes - Very low rate
LEP	90 GeV	1×10^{30}	5 nb	1/ 5	5×10^4	+ All flavors; Lifetimes - Rate
Tevatron	1.8 TeV	5×10^{30}	50 μb	1/1000	2×10^9	+ All flavors; Lifetimes - Trig; Accept; Bkgnds

Table 2. B production at e^+e^- and $p\bar{p}$ Colliders

poor signal-to-noise ratio. LEP will be also be doing a lot of physics with moving B's, and has the advantage of better signal-to-noise and the ability to trigger on essentially all interesting events. Both LEP and the Tevatron should contribute a lot to B lifetime studies and to the spectroscopy of B mesons and baryons. CESR is now running very well, and the luminosity may go even higher, so for all studies involving B_d and B_u mesons at rest it will easily dominate. So in many respects, these different accelerators are quite complementary to one another.

4 Topics in Experimental B Physics

In this section we will explore a few topics in B physics; the selection is motivated both by the desire to illustrate some of the experimental techniques, and by my personal interest in the various topics. It is not an exhaustive treatment; for more systematic coverage of topics in B physics I refer the reader the excellent review by Berkelman and Stone [42].

4.1 B Meson Masses

The masses of the B_d and B_u mesons have been precisely measured using the beam-constrained mass technique. This method exploits the fact that on the $\Upsilon(4S)$ the energy of each B meson is equal to the beam energy, because there is not enough energy available to produce any additional particles. The usual invariant mass can therefore be written as:

$$M_B^2 = \{\sum E_i\}^2 - \{\sum \vec{p}_i\}^2 = E_{beam}^2 - \{\sum \vec{p}_i\}^2.$$

The total momentum of the B meson is small, only about 345 MeV, and the momenta of the charged particles are very accurately determined. Therefore the error on the second term is small and the dominant error is due to the uncertainty in the beam energy, which is about 2 MeV at both CESR and DORIS. The beam-constrained mass technique reduces the error on the measured mass by an order of magnitude, and is also used in other analyses of B meson decays in order to improve the signal-to-noise ratio.

Beam-constrained mass fits to the B^0 and B^+ have been performed by both ARGUS [51] and CLEO [44]. Only a handful of events go into these measurements: ARGUS has about 30 events each while CLEO has about double that. The meager statistics are due to the difficulty of reconstructing these exclusive modes, which typically have small branching fractions which are further diminished when the product of the D branching fractions to reconstructable final states is folded in.

In Table 3 the 1992 PDG values for the B_d and B_u masses are tabulated, together with the most recent ARGUS and CLEO results.

	M_{B^0}, MeV	M_{B^+}, MeV	$\Delta M = M_{B^0} - M_{B^+}$, MeV
PDG 92	5278.7 ± 2.0	5278.6 ± 2.0	0.1 ± 0.8
ARGUS 90	$5279.6 \pm 0.7 \pm 2.0$	$5280.5 \pm 1.0 \pm 2.0$	$-0.9 \pm 1.2 \pm 0.5$
CLEO 92	$5278.0 \pm 0.4 \pm 2.0$	$5278.3 \pm 0.4 \pm 2.0$	$-0.4 \pm 0.6 \pm 0.5$

Table 3: B meson masses.

The PDG results are an average over the 1987 CLEO, 1990 ARGUS and 1992 CLEO results, and give almost identical values for the charged and neutral mesons. The errors on the masses are dominated by the systematic error on the beam energy, but for the mass difference, where most of this systematic error cancels, there is still some room for statistical improvement. The results are consistent, within errors, with $\Delta M = 0$.

Naively one might expect that the B_d should be slightly heavier than the B_u because the d quark is a few MeV heavier than the u quark. If we look at the mass differences in other neutral pseudoscalar mesons, we see that, in fact, there is such a pattern, with the meson containing the d quark outweighing the meson with a u quark. This is illustrated in Table 4 for the π, K and D mesons.

Pseudoscalar Meson	$\Delta M = q\bar{d} - q\bar{u}$
$M_{\pi^+} - M_{\pi^0}$	4.59 MeV
$M_{K^0} - M_{K^-}$	4.02 MeV
$M_{D^+} - M_{D^0}$	4.74 MeV

Table 4: Pseudoscalar meson mass splittings.

An obvious disclaimer should be made for the π^0 because it is in fact a superposition given by $1/\sqrt{2}(u\bar{u} - d\bar{d})$, so the fact that it follows the pattern

can only be a coincidence. Even for the K and D mesons, which do consist of heavy plus light quark combination like the B, the pattern is probably also a coincidence. These mesons are bound states, not free quarks, and the potential binding them must be taken into account. The calculation of meson masses is actually rather complicated, involving strong and electromagnetic corrections to a potential model. In a recent calculation by Flamm, *et. al* [45], a non-relativistic potential model was fit to a variety of input data to fix the form of the wave function, resulting in the meson mass predictions which are shown in Table 5.

Pseuoscalar Meson	ΔM_{str}, MeV	ΔM_{em}, MeV	ΔM_{tot},MeV
$M_{\pi^+} - M_{\pi^0}$	0	3.1	3.1
$M_{K^0} - M_{K^-}$	6.0	-1.8	4.2
$M_{D^+} - M_{D^0}$	0.7	2.9	3.6
$M_{B^0} - M_{B^+}$	-0.2	-1.3	-1.5

Table 5: Predictions of Flamm [45] for pseudoscalar meson mass splittings.

From this we see that the corrections are different for each meson, conspiring to result in $\Delta_M \approx 4$ MeV for the π, K and D mesons but yielding a predicted value of $\Delta_M = -1.5$ MeV for the B system, which is in fair agreement with the most recent experimental data.

The closeness of the charged and neutral B meson masses implies that the ratio of charged to neutral B meson production, f_+/f_0, discussed in section 3.1, is also close to unity except for the effects of the Coulomb interaction, which favor charged meson pair production slightly. Future improvements in ΔM are very likely as CLEOII is accumulating a very large data set and will be able to reduce the statistical error on this measurement by increasing the number of fully reconstructed B decays.

Finally, a technical point regarding the masses. In the neutral B meson system the weak eigenstates do not coincide with the flavor eigenstates due to flavor oscillations, or mixing. The flavor eigenstates, the B^0 and the $\bar{B}^0$ ($= \bar{b}d$ and $b\bar{d}$) must have equal masses and lifetimes, according to the CPT theorem, but the weak eigenstates, B_1 and B_2 have different masses and different lifetimes. The mass difference in the weak eigenstates is on the order of 10^{-10} MeV and is obviously too small to be measured directly;

however it has been determined from the rate of $B^0\bar{B}^0$ mixing. While very small by any usual standards, this mass difference is very large compared to the analagous mass difference in the neutral K-meson system, where it is on the order of 10^{-12} MeV. On the other hand, there is a very large lifetime difference between the weak eigenstates in neutral K-meson system, which is why the weak eigenstates are known as $K_{L(ong)}$ and $K_{S(hort)}$. By contrast, in the B system, the lifetime difference is expected to be too small to ever be experimentally measured. So perhaps we should call the B weak eigenstates $B_{H(eavy)}$ and $B_{L(ight)}$.

4.2 B Lifetime

The measurement of the B lifetime provides information about the CKM parameters V_{cb} and V_{ub}, and tests assumptions about the dominance of spectator diagrams in B decays. In the D-meson system the unequal lifetimes measured for the D^+ and the D^0 revealed the importance of non-spectator effects in D decays. The measured D^+ lifetime is in fact about twice as long as the D^0 lifetime, and this has been attributed to the fact that W exchange is allowed for the D^0 , increasing its total width, while this diagram is not allowed for the D^+. In addition, both internal and external spectator diagrams are possible for the D^+ though not for the D^0; destructive interference between these diagrams is thought to reduce the total width of the D^+. Because the b quark is so much heavier than the c quark, it is expected that the naive spectator model should be a much better approximation, and that non-spectator effects will be small.

There are two types of B lifetime measurement: the average B hadron lifetime, and the flavor-tagged B lifetime. Experimentally, the simplest is the average B hadron lifetime, in which different flavors are not distinguished, and the average is taken over all produced B hadrons, weighted by their statistical share in the final event sample. The advantage of this technique is that by using a high p_t lepton tag one can obtain a fairly pure sample of B hadrons with good statistics. The disadvantage, of course, is that one is not sensitive to lifetime differences between different flavors of B mesons, or even between mesons and baryons. Therefore the comparison with theory must rely on the assumption of spectator dominance. In addition, different measurements may contain slightly different mixtures of B hadrons depending on the type of accelerator, the center-of-mass energy and the selection criteria. Flavor-tagged lifetimes are experimentally more challenging because the B hadron must be at least partially reconstructed or tagged by identifying characteristic decay products. This is in principle a superior measurement but so far such measurements have been statistically limited.

The average B hadron lifetime has been measured by many experiments at PEP, PETRA and LEP. The majority of these measurements employ the signed impact parameter technique so let us briefly review this method. The measurement is performed only in the xy plane, defined as the plane normal to the beam-line and intersecting it at z=0. Note that in e^+e^- storage rings the beam spot is typically much larger in the horizontal (x) direction than in the vertical (y) direction due to synchrotron radiation, which is emitted tangential to the beam, while for hadron colliders and single-pass e^+e^- colliders the beam spot is usually round. As illustrated in Fig. 16, the signed impact parameter is obtained by measuring the 'miss distance' between the average beam spot position and the extrapolated track of a high p_t track. Some experiments have improved on this by measuring the the primary vertex on an event-by-event basis, reducing the error due to the size of the beam spot. The high p_t track is often a lepton, which is also used to tag the event.

The impact parameter is defined by

$$\delta = \gamma\beta c\tau \sin\alpha \cdot \sin\theta,$$

where α is the angle between the lepton track and the jet axis, θ is the polar angle, $\gamma\beta = p_B/M_B$ and τ is the lifetime to be determined. The sign is determined by measuring the jet axis of the event and determining where the high p_t track crosses the jet axis: if it crosses before the beam spot then the impact parameter is positive, indicating that it could indeed have originated from the decay in flight of a long lived particle originating from the beam spot. If it crosses the jet axis behind the beam spot the impact parameter is negative; sources of negatively-signed impact parameters include tracking resolution, imperfect jet axis determination as well as backgrounds in the event sample.

Now, naively, one might expect δ to increase linearly with the momentum of the B meson, resulting in larger average impact parameters at higher c.m. energy. In fact, this is not quite the case. There is a saturation effect due to the fact that, as $\gamma\beta$ increases, $\sin\alpha$ decreases approximately like $1/\gamma\beta$ for $\beta \approx 1$; see Fig. 17 for the average impact parameter vs γ_B. At PEP and PETRA energies the average impact parameter is on the order of 400 μm, while at LEP and SLC, where the center of mass energy has increased by three-fold, the average impact parameter increases by only about 30% to approximately 550 μm.

In addition to the small increase in the average value of the impact parameter, there is another advantage to measuring B lifetimes at the Z^0: the uncertainty due to the B meson momentum, which is only measured on average, is reduced as one approaches the asymptotic value of δ_{max}. The small beam spot size at LEP and SLC also helps; at LEP it is about 10 μm in the

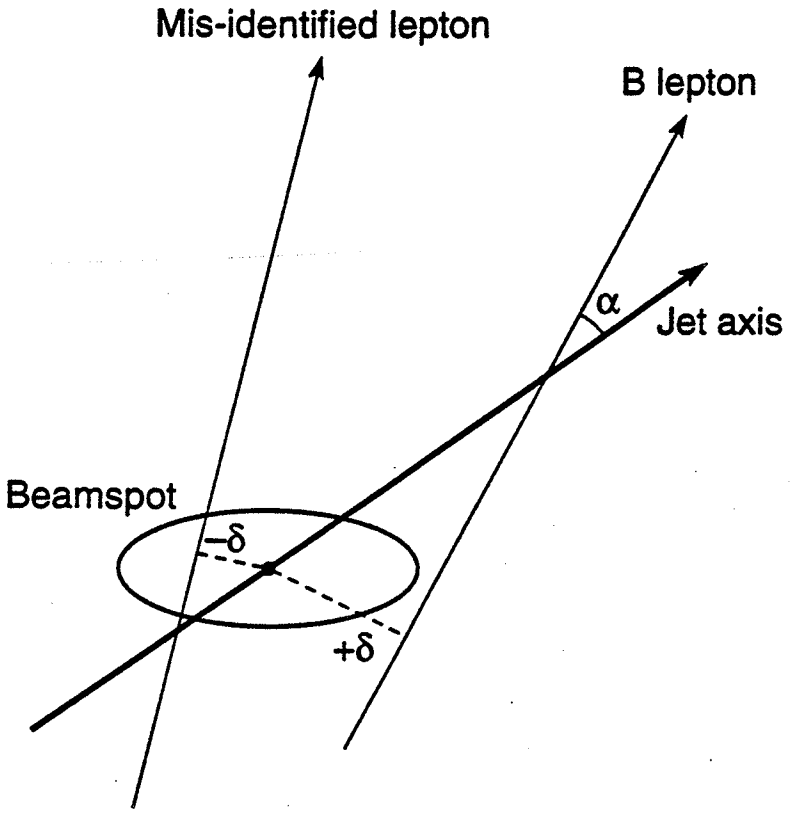

Figure 16: The determination of the impact parameter, δ, in the xy plane.

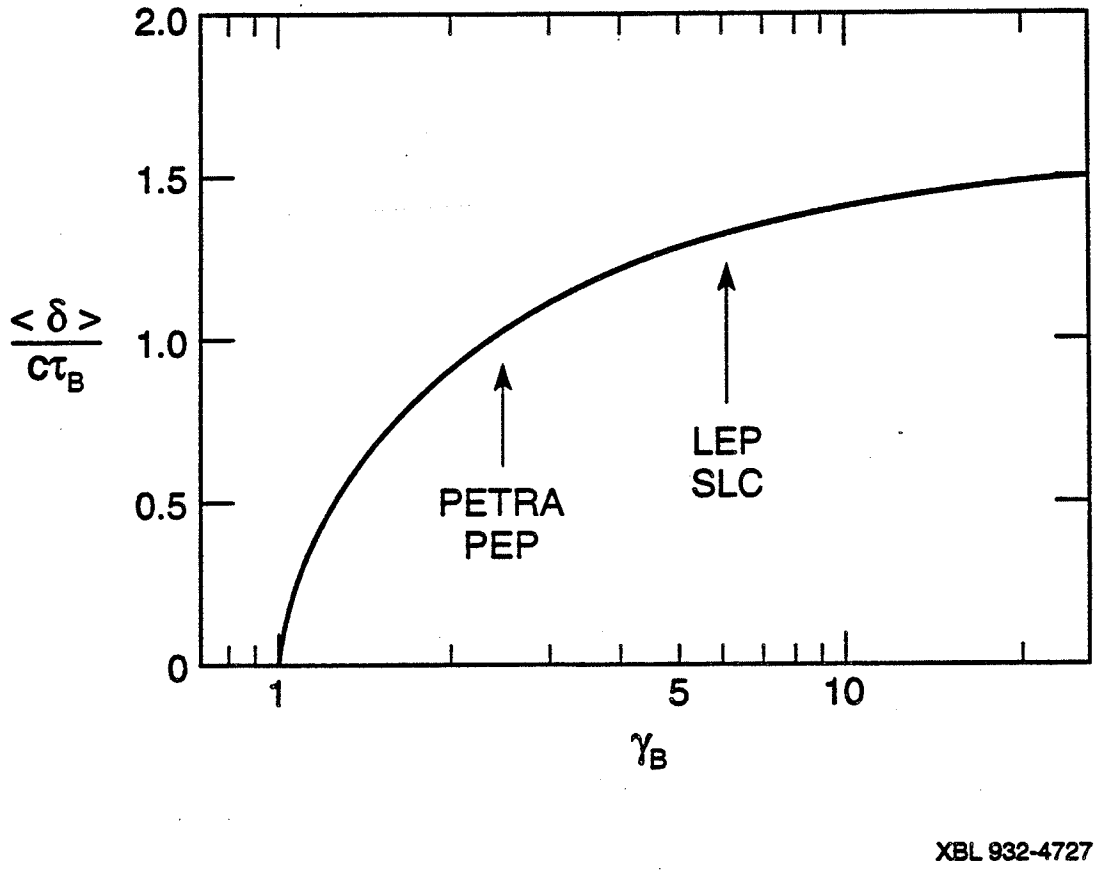

Figure 17: The mean impact parameter in units of $c\tau_b$ vs. γ of the B hadron.

vertical direction and 200μm in the horizontal direction, while at SLC it is just under 2μm in both directions.

In Fig.18 the impact parameter distribution from ALEPH [47] is shown for events which were chosen to have a lepton with $p_t > 2$ and $p > 5$ GeV; the distribution is roughly Gaussian, with a long tail due to the finite decay length of the B hadrons. A fit is performed to this distribution, taking into account the expected backgrounds due to charm, mis-identified leptons, and decays in flight. The impact parameter in this measurement has a resolution of about 200 μm. There are a total of almost 3000 events, and the measured B hadron lifetime is $1.29 \pm 0.06 \pm 0.10$ ps.

In Fig. 19 a new, preliminary result from ALEPH [48] is shown; in this measurement they have used a silicon vertex detector to improve the impact parameter resolution to 60 μm. (Part of this improvement is due to a new method of estimating the primary vertex on an event-by-event basis, reducing the error on the horizontal component from 200 μm to 50 μm.) The impact parameter distribution is narrower, the tail is much more pronounced and the backgrounds are reduced from 27% to 10%. The background reduction is mainly due to a new jet algorithm which takes into account neutral particles, allowing the p_t of the lepton with respect to the jet axis to be more accurately measured. The net effect of all these improvements in the analysis combined with the precision of the silicon vertex detector has reduced the error on the B hadron lifetime by about a factor of 2 over the previous measurement. The updated result is an average lifetime of $1.49 \pm 0.03 \pm 0.06$ ps, based on an event sample of almost 5000 events. The new result is about 1.5 σ longer than the previous result, which was more or less consistent with the world average. At present, three of the four LEP detectors have installed silicon vertex detectors and are acquiring large new data sets. We can expect that a new round of lifetime measurements from LEP will soon be published when these data have been analyzed.

In Fig. 20, the measurements of the average B hadron lifetime which use the signed impact parameter technique for high p_t leptons are plotted. (The world average does not include the most recent data from ALEPH.) The early measurements from PEP and PETRA have rather large errors compared to the more recent measurements from LEP. There is an interesting trend in that the average measured value seems to be increasing with time.

There are techniques other than the signed impact parameter which have been used to determine the average B hadron lifetime. Recently, a new technique has been employed at LEP using J/Ψ's , in which they are reconstructed in the decay to e^+e^- or $\mu^+\mu^-$. The vertex of the J/Ψ provides a 3-dimensional space point which coincides with the decay point of the B hadron; using this vertex information the decay length is determined. The

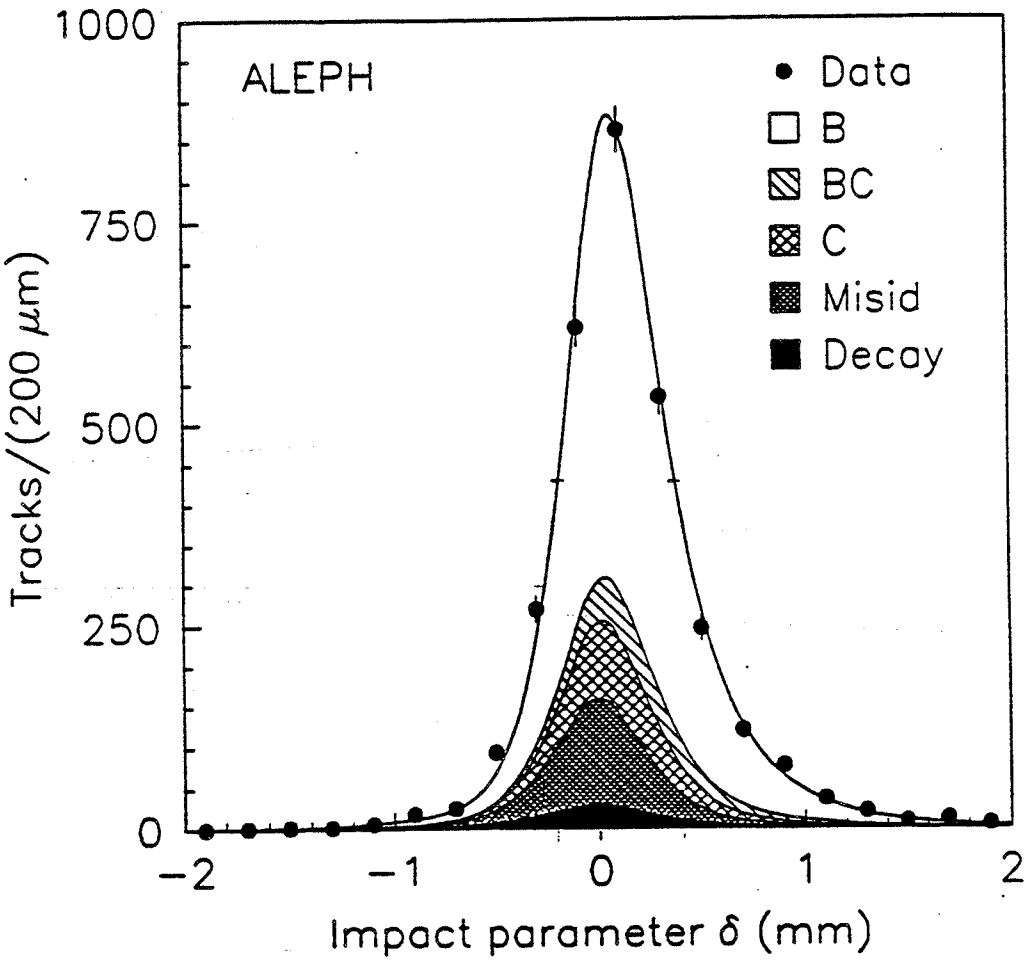

Figure 18: The signed impact parameter distribution from ALEPH in 1991, from ref. [47].

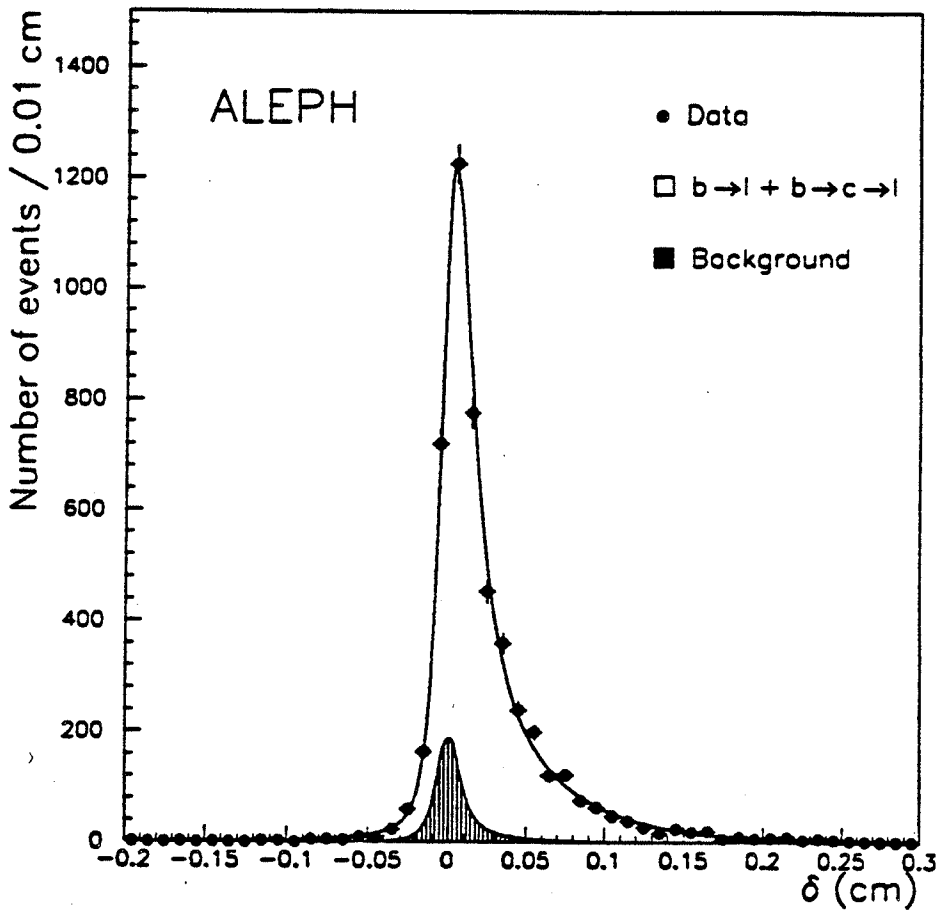

Figure 19: The signed impact parameter distribution from ALEPH in 1992, from ref. [48].

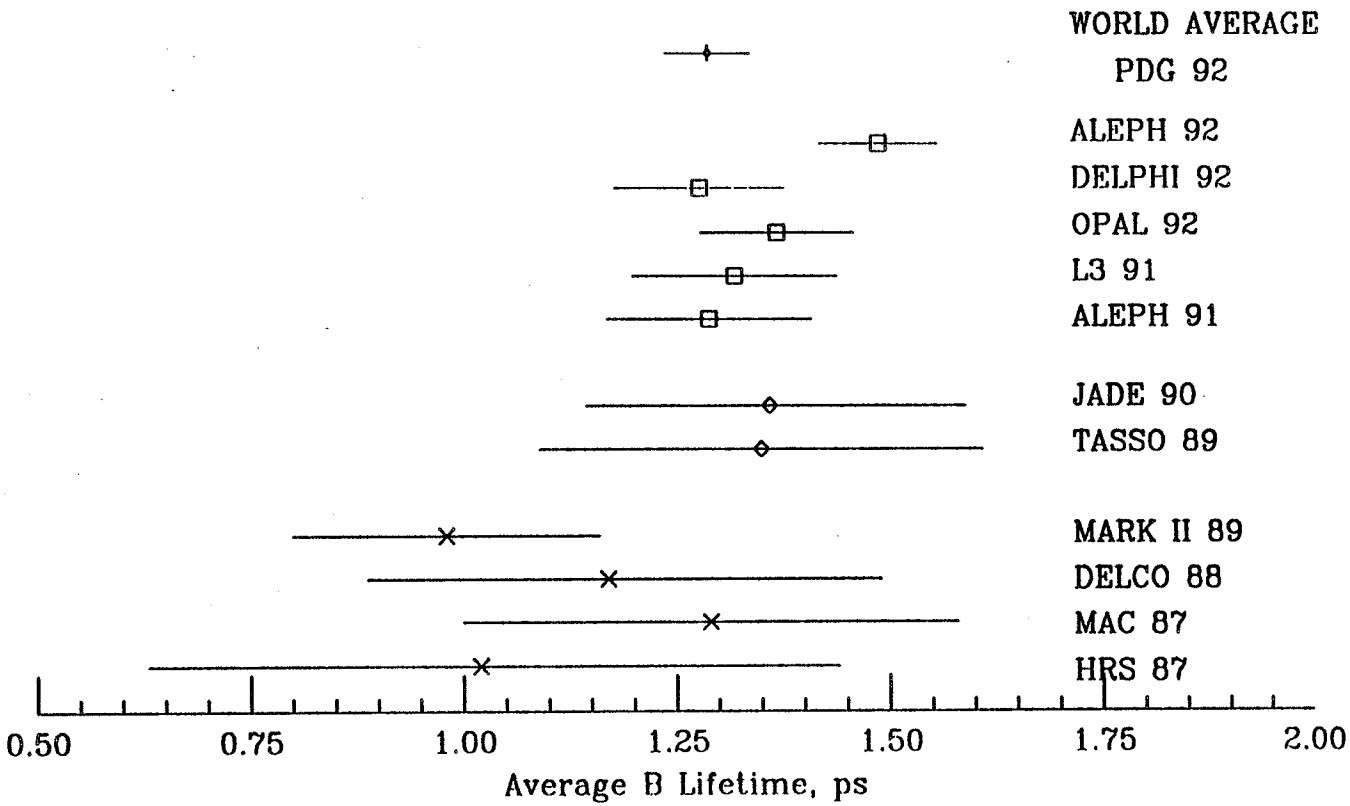

Figure 20: Average B hadron lifetimes measurements using lepton impact parameter.

3-dimensional decay length is quite long, averaging over 2 mm. ALEPH has obtained an average B hadron lifetime of $1.35^{+0.19}_{-0.17} \pm$0.05 ps using this technique, and DELPHI reports a similar result of $1.32^{+0.31}_{-0.25} \pm 0.15$ ps. This technique will also be useful at hadron colliders, where J/ψ's are used to trigger on B events.

In addition to measuring an average B hadron lifetime with J/ψ's, ALEPH has reported a signal of 5 events in the exclusive channel $B^+ \to J/\psi K^+$. Although they have not reported a lifetime for this handful of flavor-tagged B mesons, we can anticipate that with improved statistics this technique will be employed at LEP and perhaps also at the Tevatron to measure the B^+ and B^0 lifetimes individually.

The first flavor-tagged measurement of the B^0 lifetime was made in 1990 by the MarkII collaboration [49], using data from PEP. They identified events of the type $B^0 \to D^{*-} l^+ \nu$. In order to enhance statistics the D^{*-} was not fully reconstructed, but was tagged using the bachelor pion technique. This technique exploits the fact that in the decay $D^{*-} \to \bar{D}^0 \pi^-$, the quantity $\Delta m = m(D^{*-}) - m(\bar{D}^0)$ is only 145 MeV. Low momentum tracks ($p < 1.0$ GeV) were taken as candidates for the bachelor pion and Δm was computed, using the other charged tracks (excluding the lepton) and photons in the B jet to make the $\bar{D}^0$ candidate. They observed an enhancement at $\Delta m = 145$ MeV for the correct pairing of π^- with l^+, and none for the wrong-sign combination, indicating a signal for the D^{*-}. The $D^{*-} l^+$ pairing was in turn evidence for the B^0, because a B^+ decays dominantly to $D^{*0} l^+ \nu$. The D^{*0} in turn decays only to $D^0 \gamma$ and $D^0 \pi^0$, and not to $D^+ \pi^-$, so the bachelor pion technique is a good method of identifying B^0's. In fact the estimated purity of the B^0 sample was 93%, which is very good. Unfortunately the statistics were low, and only 15 events were obtained. Fitting the impact paramter distribution gave a B^0 lifetime of $1.20^{+0.52+0.16}_{-0.36-0.14}$ ps, which is consistent with the average B hadron lifetime within errors. Although this particular measurement was limited by statistics, there is no reason that it cannot be applied at LEP where there are many more B's.

There is also an indirect way of measuring the ratio of the B_d to the B_u lifetime. This technique takes advantage of the fact that the semi-leptonic decay width for the two species should be identical. The ratio of the lifetimes is then proportional to the ratio of the semi-leptonic branching ratios:

$$\frac{\tau_+}{\tau_0} = \frac{\Gamma_0}{\Gamma_+} = \frac{\Gamma(B^0 \to D^{*-} l^+ \nu)}{Br(B^0 \to D^{*-} l^+ \nu)} \cdot \frac{Br(B^+ \to \bar{D}^{*0} l^+ \nu)}{\Gamma(B^+ \to \bar{D}^{*0} l^+ \nu)}$$
$$= \frac{Br(B^+ \to \bar{D}^{*0} l^+ \nu)}{Br(B^0 \to D^{*-} l^+ \nu)}$$

Using this technique, CLEO and ARGUS have measured τ_+/τ_0. The

CLEO result [50] is $(0.89 \pm 0.19 \pm 0.13) \cdot f_0/f_+$, and the ARGUS result [51] is $(1.00 \pm 0.23 \pm 0.14) \cdot f_0/f_+$. There is an additional uncertainty due to the our lack of knowledge concerning f_+/f_0, the ratio of charged to neutral B production. Both results are consistent with unity within the errors.

4.3 Inclusive Semileptonic Decays

The semileptonic branching fraction for B's can be naively determined by assuming spectator dominance and calculating the W decay rates. In Table 6 the allowed W decays, and the corresponding color and phase space factors are shown.

Decay	Color Factor	Phase Space Factor	Relative Rate
$W^- \to \bar{u}d$	3	1.0	3.0
$W^- \to \bar{c}s$	3	0.3	0.9
$W^- \to e^-\nu$	1	1.0	1.0
$W^- \to \mu^-\nu$	1	1.0	3.0
$W^- \to \tau^-\nu$	1	0.3	.3
Total			6.2

Table 6: Relative W partial decay rates in spectator B decay.

Using the results in Table 6, we would calculate a total leptonic branching fraction of 1.0/6.2 or 16% for the electronic and muonic branching fractions. QCD corrections increase the width into all hadronic final states, decreasing the semi-leptonic branching fraction to about 13%. However, the experimental measurements of the semi-leptonic branching fractions are somewhat lower; the Particle Data Group quotes the average value as $10.3 \pm 0.5\%$ for $B \to e^-\nu_e X$ and $10.7 \pm 0.5\%$ for $B \to \mu^-\nu_\mu X$.

Before going into this discrepancy and discussing possible explanations, let us review how the semi-leptonic branching ratio is measured. On the $\Upsilon(4S)$ one begins with the standard hadronic event selection, with the additional requirement of an electron or a muon. ARGUS requires the lepton to have $|p|$ >1.4 GeV, while CLEO accepts electrons with momenta above

0.5 GeV and muons above 1.5 GeV (the minimum momentum required for a muon to penetrate their muon system). The background contributions from the continuum, from mis-identified leptons, and from leptons originating from the processes $B \to J/\psi + X$ and $B \to \tau + X$ are subtracted, and the spectrum is corrected for tracking and lepton identification inefficiencies. The resulting lepton momentum spectra is then fitted to the sum of all contributions: $b \to cl\nu$, $b \to c \to sl\nu$, as well as $b \to ul\nu$. The shape of the fit is taken from theory, except for the contribution from $b \to c \to sl\nu$, where experimentally measured lepton momentum spectra from D decays are used.

The difficulty is in the model-dependence of the fit. There are several models for B semi-leptonic decay; and they all tend to give slightly different results. The most popular models include the free quark model of Altarelli *et. al.* (ACCM) [52], which treats the b quark decay very much like muon decay, and the Isgur-Scora-Grinstein-Wise (ISGW) [53] model, which is based on a form factor calculation which takes into account the fact that the B meson does not decay to a continuum of states but into a few exclusive final states, each with a characteristic lepton momentum spectrum. The models of Wirbel, Stech and Bauer (WSB) [54] and of Korner and Schuler (KS) [56] are also based on exclusive final states and assume a relativistic bound state for the B meson. However they do not include decays involving the D**, so these models are only applicable in the high momentum region, above about 1.9 GeV.

More recently, there has been a theoretical effort which goes under the name of Heavy Quark Effective Theory (HQET), which was started by Wise and Isgur [57]. In this theory, one takes the limit in which the mass of the b quark goes to infinity and new symmetries in both flavor and spin arise,which allow one to use universal form factors. Thus the form factors for B and D decay are related in a way which can be calculated. There is great hope that this new theory will allow more accurate modeling of semi-leptonic B decays, and hence a better determination of the semi-leptonic branching ratio and also of V_{cb}.

Once one has chosen a model to fit the lepton momentum spectrum and extracted the inclusive B semi-leptonic branching fraction, the CKM parameter V_{cb} can be determined through its relationship to the semi-leptonic width:

$$\Gamma(b \to Xl\nu) = \frac{G_F^2 M_b^5}{192\pi^3}\{f_{cb}|V_{cb}|^2 + f_{ub}|V_{ub}|^2\}.$$

In a measurement of $|V_{cb}|$ one can neglect $|V_{ub}|$ to first order. The phase space factor f_{cb} is calculated to be equal to 0.49. A large systematic uncertainty is introduced by the strong dependence on the b quark mass. In addition, one must use the B lifetime to relate the semi-leptonic width to the measured

semi-leptonic branching fraction:

$$\Gamma(b \to Xl\nu) = \frac{Br(B \to Xl\nu)}{\tau_b}.$$

The fact that the B lifetime has been precisely measured only for a mixture of B hadrons is another source of systematic uncertainty, estimated by CLEO to be on the order of 20%.

The results of CLEO [58], ARGUS [59] and the Crystal Ball [60] for two of the phenomenological models discussed above are shown in Table 7.

	CLEO	ARGUS	Crystal Ball
ACCM			
Br,%	$10.5 \pm 0.2 \pm 0.4$	$10.15 \pm 0.4 \pm 0.2$	12.0 ± 0.5
V_{cb}	$0.048 \pm 0.002 \pm 0.005$	0.047 ± 0.004	0.053 ± 0.009
ISGW			
Br,%	$11.2 \pm 0.3 \pm 0.4$	9.9 ± 0.4	11.9 ± 0.4
V_{cb}	$0.042 \pm 0.002 \pm 0.004$	0.046 ± 0.006	0.042 ± 0.005

Table 7: The inclusive semi-leptonic B branching fraction and V_{cb}.

From these results it is clear that model dependence dominates the systematic error on the results.

One interesting aspect of the CLEO measurement is that the ISGW model does not give a good fit to their data unless they increase the contribution for final states involving a D^{**} from the theoretical value of 13% up to 32%. The CLEO data and the two fits to the ISGW model are shown in Fig. 21, taken from ref. [58]. From the figures it is seen that the observed lepton momentum spectrum is softer than the default ISGW model with 13% D^{**} predicts. Because leptons from final states involving the D^{**} are softer than those with a D^* or D, increasing the D^{**} fraction brings the model into better agreement with the data. This excess of soft leptons in the CLEO data results in a larger semi-leptonic branching ratio than ARGUS finds, because they have a higher minimum lepton momentum requirement. The Crystal Ball measurements are for electrons only; they find a slightly larger value of the semi-leptonic branching ratio than either CLEO or ARGUS, which use both electrons and muons and find consistent results for the two channels.

The inclusive B hadron semileptonic branching fraction has also been measured at PEP, PETRA and LEP, where the measurement represents an

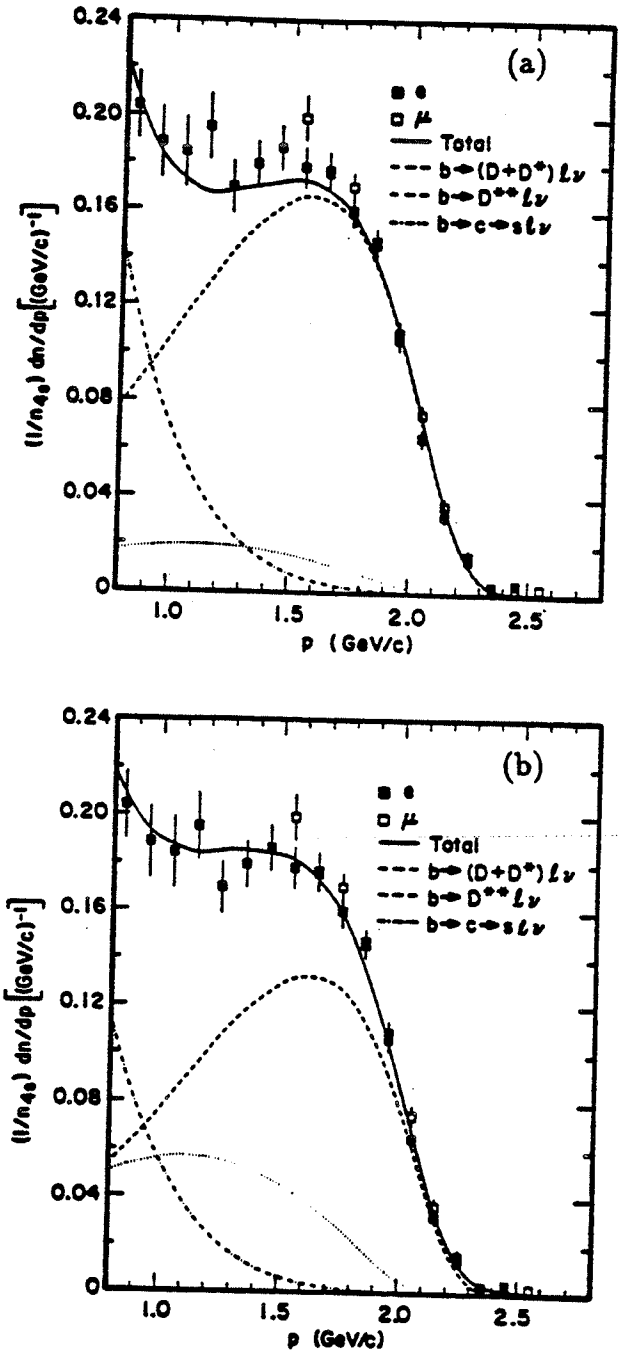

Figure 21: The inclusive lepton spectrum from CLEO, with fits to the ISGW model with (a) 13% D^{**}, and (b) 32% D^{**} contributions, from ref. [58].

average over all B hadrons. If one takes the average of all these measurements the result is $11.3 \pm 0.4\%$ [42], which is a little higher than the average of the $\Upsilon(4S)$ measurements though consistent within the errors.

The measured inclusive semi-leptonic branching ratios on both the $\Upsilon(4S)$ and at higher energies are all systematically lower than 13%, the value predicted by the naive spectator model with QCD corrections. A recent paper by Altarelli and Petrarca [61] suggest that this could be due to a contribution to B^0 decay from W exchange with gluon emission, increasing the B^0 width and reducing the B^0 semileptonic branching fraction. This would imply that the B^0 lifetime is shorter than the B^+ lifetime, but the constraints on τ_+/τ_0 from CLEO and ARGUS limit this difference to 20% or less. If we assume that $\tau_+/\tau_0 = 1.2$, this would imply that the semi-leptonic branching fraction of the B^0 is decreased by 20%, reducing the average semileptonic branching fraction measured on the $\Upsilon(4S)$ by 10%. In this way the naive expectation of 13% can be reduced to 11.7%, which gives better but not perfect agreement with the experimental results. More precise measurements of the flavor-tagged B lifetimes will allow us to test this hypothesis.

The lepton momentum spectrum in inclusive semileptonic B decays also provides information on the CKM element V_{ub}. The analysis is very similar to what we have already discussed for the determination of V_{cb}, except that in this case we are primarily interested in the very high momentum part of the distribution. In the region above about 2.2 GeV, decays from $b \to c l \nu$ cannot contribute; only the decay $b \to u l \nu$ is kinematically allowed. Of course there is still a contribution from the continuum background but that is estimated by running off resonance. Both CLEO [62] and ARGUS [63] have reported evidence for an excess of leptonic events in the high momentum region. The lepton spectra from CLEO and ARGUS are shown in Fig. 22 with the fits to $b \to c l \nu$ superimposed. Both show an excess of about 70 events in the high momentum region, which is taken as evidence for $b \to u l \nu$ decays. Once again one needs a model in order to fit the lepton momentum spectrum and once again model dependence will dominate the systematic error on the extraction of the CKM matrix element V_{ub}. This is illustrated by the results tabulated in Table 8. However large the uncertainties are on the measured value of $|V_{ub}|$, there does seem to be good evidence that it is non-zero, and this is very important since if any element of the CKM matrix is zero there is no natural explanation of CP violation within the Standard Model. In fact ARGUS [64] has observed one remarkable event in which they have reconstructed both B decays and they observe $\bar{B}^0 \to D^{*+}\rho^-$ and $B^0 \to \bar{B}^0 \to \mu^-\pi^+\nu$. This event therefore involves both mixing and $b \to u$ so it is truly unusual and provides us with concrete evidence that $V_{ub} \neq 0$.

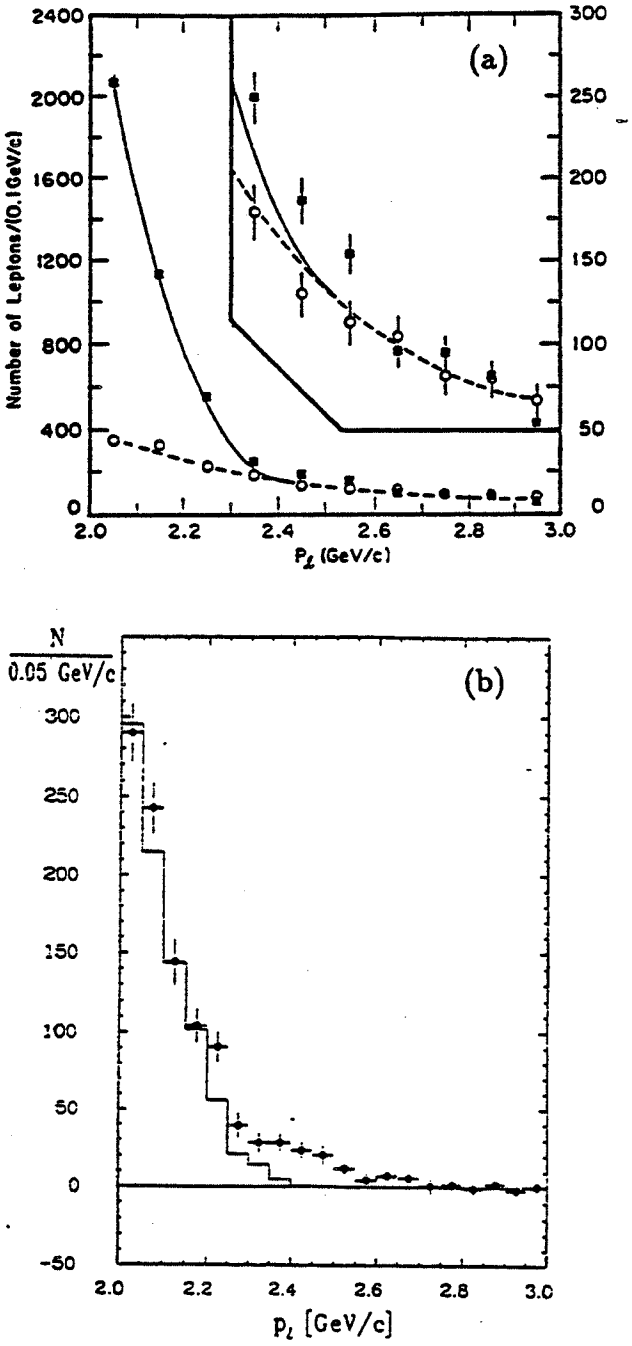

Figure 22: Endpoint of the lepton spectrum from (a) CLEO and (b) ARGUS showing excess due to $b \rightarrow u$ transitions (ref. [62] and [63]).

	ARGUS	CLEO
ACCM	0.11 ± 0.012	0.09 ± 0.011
ISGW	0.20 ± 0.023	0.15 ± 0.020
WSB	0.13 ± 0.015	0.11 ± 0.018
ACCM	0.11 ± 0.012	0.09 ± 0.011

Table 8: Results from various models for $|V_{ub}|/|V_{cb}|$.

4.4 Exclusive Semileptonic Decays

Exclusive semileptonic B decays are of interest because they provide some important checks on the theory used in the inclusive semileptonic analyses, and also because they can in principle provide a less model-dependent determination of V_{cb} and V_{ub}.

Because these final states involve a neutrino, they cannot be fully reconstructed in the usual sense. However there is a trick called the missing mass technique which is used to obtain a clean sample of decays of the type $B \rightarrow (D, D^*, D^{**})l\nu$. The lepton and the D candidate are identified. One then reconstructs the missing mass, defined by

$$M^2_{miss} = (E_B - E_D - E_l)^2 - (\vec{p_B} - \vec{p_D} - \vec{p_l})^2.$$

The missing mass is just the mass of the unobserved neutrino, and should therefore equal 0 if all of the other decay products have been correctly identified and associated. In this expression the B meson energy is taken to be equal to the beam energy, but the B meson momentum vector is not known and is usually set to zero, introducing some smearing of the missing mass distribution. The ARGUS missing mass distribution for the decay mode $B^- \rightarrow D^{*0}l^-\nu$ is shown in Fig. 23. The data have been background-subtracted and show a clear signal at M^2_{miss}=0.

Using this technique, both ARGUS [66, 67, 68, 69] and CLEO [50, 65] have observed exclusive semi-leptonic B decays and have measured the semileptonic branching fractions to D and D^*. The most recently published values are listed in Table 9.

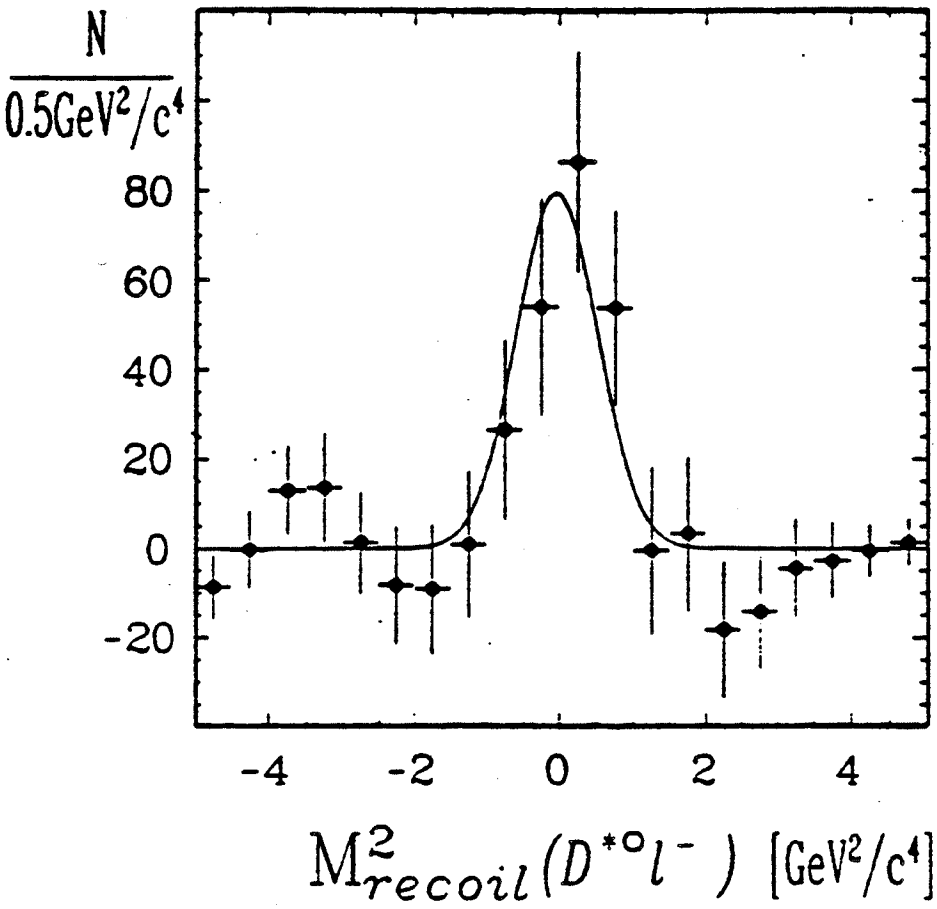

Figure 23: Missing mass distribution from ARGUS for $B^- \to D^{*0} l^- \nu$ from ref. [69].

	CLEO	ARGUS
$Br(B^- \to D^0 l^- \nu)$	$(1.6 \pm 0.6 \pm 0.3)\%$	
$Br(B^- \to D^{0*} l^- \nu)$	$(4.1 \pm 0.8^{+0.8}_{-0.9})\%$	$(5.8 \pm 1.4 \pm 1.3)\%$
$Br(\bar{B}^0 \to D^+ l^- \nu)$	$(1.8 \pm 0.6 \pm 0.3)\%$	$(1.8 \pm 0.6 \pm 0.5)\%$
$Br(B^0 \to D^{+*} l^- \nu)$	$(4.6 \pm 0.5 \pm 0.7)\%$	$(5.4 \pm 0.9 \pm 1.3)\%$

Table 9: Measured exclusive semi-leptonic B branching ratios.

There are some interesting points to be drawn from these measurements. First of all, the measured value of the ratio of the vector (D^*) decays to the pseudoscalar (D) decays is $2.6^{+1.1+1.0}_{-0.6-0.8}$ from CLEO and $3.3^{+3.7}_{-1.1}$ from ARGUS, both of which are consistent with the naive expectation of 3 and with the theoretical predictions which range from about 2.3 to 3.1 [53, 55, 56].

Next, instead of taking the ratio, let's add them up and compare the total, averaged over the charged and neutral B mesons, to the total inclusive semileptonic branching ratio. CLEO reports $(6.1 \pm 0.6 \pm 1.1)\%$, while ARGUS finds $(7.2 \pm 1.1 \pm 1.4)\%$. In both cases they do not saturate their observed inclusive rates of just over 10%. We know that most of the semileptonic B decays are to charmed final states. In fact CLEO has measured the inclusive charm content in semi-leptonic decays and found $0.93 \pm 0.11 \pm 0.11$ D's per semileptonic B decay. So if we measure the fraction of B's that decay to the exclusive D and D^* channels, and divide by the inclusive semileptonic rate to charm, we find that only $64 \pm 10\%$ of the exclusive decays are accounted for, according to the CLEO results. The remaining one-third are most likely decays to D^{**} or to nonresonant $D + n\pi$ final states. This evidence is in agreement with the 32% D^{**} which CLEO must assume in order to fit the low-momentum part of the inclusive lepton spectrum, as discussed above.

Next we would like to use these measured exclusive semileptonic branching ratios to extract $|V_{cb}|$. The most accurate measurement of $|V_{cb}|$ should come from the exclusive modes because the inaccuracy introduced by the factor m_b^5, necessary for the inclusive modes, is replaced by a form factor (one for $B \to Dl\nu$ and three for $B \to D^* l\nu$) which, though subject to theoretical uncertainty, should be more precisely known. Table 10 below, taken from a review by Berkelman and Stone [42] summarizes the results for a variety of models, using the average measured branching fractions.

Model	$B \to Dl\nu$	$B \to D^* l\nu$	Average
ISGW	0.36 ± 0.005	0.039 ± 0.004	0.038 ± 0.003
KS	0.42 ± 0.005	0.039 ± 0.004	0.040 ± 0.003
WSB	0.42 ± 0.005	0.042 ± 0.004	0.042 ± 0.003

Table 10: $|V_{cb}|$ from exclusive semileptonic B decays.

The model dependence is still present but is much less dramatic than in the inclusive semileptonic decays. There is still a large uncertainty due to the reliance on τ_b which is precisely measured only as an average over B hadrons but not yet for B^0 or B^+. This provides an interesting example of how progress on different fronts of B physics are strongly coupled, and is one more reason to look forward to more accurate flavor-tagged lifetime measurements from LEP or from the Tevatron.

4.5 $\bar{B}B$ Mixing

Our next topic is $\bar{B}B$ mixing. Both the B_d and the B_s can mix through the box diagram shown in Fig. 3e. The mixing in each system is characterized by by $\Delta M/\Gamma$, where ΔM is the mass difference between the weak eigenstates B_H and B_L (for heavy and light), and Γ is the average total width. The quantity $\Delta M/\Gamma$ is often referred to as x_d, for the B_d, or x_s for the B_s. From the box diagrams for mixing we see that the mixing amplitude will depend on the CKM matrix element V_{td}, in the case of B_d mixing, and on V_{ts}, in the case of B_s mixing. The ratio of mixing in the B_s system to mixing in the B_d system is proportional to the square of the ratio of these CKM matrix elements:

$$\frac{x_s}{x_d} \approx \frac{|V_{ts}|^2}{|V_{td}|^2}.$$

From unitarity of the CKM matrix it has been estimated that x_s is at least 10 and possibly more than 20 times greater than x_d. The mixing amplitudes for both B_s and B_d are also related to the top quark mass, because the diagram with a top quark in the loop gives the dominant contribution to the amplitude. The heavier the top quark mass, the larger the mixing amplitude, so mixing measurements have also been used to set lower limits on m_t.

There are two quantities which are commonly used to describe the rate

of mixing. One is given by

$$r_{d,s} = \frac{\Gamma(B_{d,s} \to \bar{B}_{d,s} \to l^- X)}{\Gamma(B_{d,s} \to l^+ X)},$$

The quantity r is bounded between 0 and 1 and is commonly used for mixing measurements on the $\Upsilon(4S)$. The other quantity is

$$\chi_{d,s} = \frac{\Gamma(B_{d,s} \to \bar{B}_{d,s} \to l^- X)}{\Gamma(B_{d,s} \to l^+ X) + \Gamma(B_{d,s} \to \bar{B}_{d,s} \to l^- X)}.$$

χ is bounded between 0 and 0.5, and is related to r by

$$\chi_{d,s} = \frac{r_{d,s}}{1 + r_{d,s}}.$$

We will use the quantity χ in this discussion, since it is more universally used; it is related to the mixing parameter x by

$$\chi_{d,s} = \frac{x_{d,s}^2}{2 + 2x_{d,s}^2}.$$

Experimentally, one determines the mixing rate by comparing the rates for like-sign and unlike-sign di-lepton events. This ratio depends upon where the measurement is performed. On the $\Upsilon(4S)$ the $B_d\bar{B}_d$ pair is produced in a $J^P = 1^-$ state, and as one B mixes the other mixes in phase with it in order to preserve this quantum configuration. At the moment when the first meson decays as either a B_d or a $\bar{B}_d$, the other meson must be in the other state. It may then mix independently, because the decay of the first B breaks the quantum coherence. This situation on the $\Upsilon(4S)$ results in a very simple relationship between the observed number of like- and unlike-sign dilepton events and the quantity χ_d:

$$\chi_d = \frac{N(l^\pm l^\pm)}{N(l^\pm l^\pm) + N(l^+ l^-)}.$$

The di-lepton rates must of course be corrected for the contribution from B^+B^- production, for cascade leptons from charm, and for mis-identified leptons. The average value of χ_d from from ARGUS [70] and CLEO [71] is $\chi_d = 0.153 \pm 0.031$, which corresponds to $x_d = 0.67 \pm 0.10$ [72]. These values are calculated assuming $f_+/f_0 = 1$ and $\tau_+/\tau_0 = 1$; the result is sensitive to these assumptions because of the need to correct for di-leptons from B^+B^- production, and because the semi-leptonic branching ratio is proportional to the lifetime.

The situation is very different when B's are produced off the $\Upsilon(4S)$. There is no quantum coherence and both B's mix independently. In many cases, a B^0 will be produced together with a charged B or a B baryon, neither of which can mix at all. In addition, it is possible to produce both B_d and B_s mesons, and the latter mixes at a much higher rate. From the measured value of x_d of around 0.7 we can estimate that x_s is at least 5, and very likely larger than 10. The implication is that χ_s will then be very close to the upper limit of 0.5. The measured mixing rate therefore depends on the produced fraction $f_{d,s}$ of B_d and B_s. There will also be backgrounds due to leptons from the sequential decay $b \to c \to l$ and from direct charm decays. The experimental quantity which is measured, $\chi = f_d\chi_d + f_s\chi_s$, is an average over B_d and B_s mixing weighted by their production fractions. In the simplest case, if we assume that the sources of background are negligible (though this is not the case experimentally), χ is related to the di-lepton rates by:

$$\frac{N(l^{\pm}l^{\pm})}{N(l^{+}l^{-})} = \frac{2\chi(1-\chi)}{(1-\chi)^2+\chi^2}.$$

χ has been measured at LEP [73, 74, 75] as well as at hadron colliders [76, 77]. The measurements are summarized in Table 11.

Experiment	$\chi = f_d\chi_d + f_s\chi_s$
UA1	$0.145 \pm 0.035 \pm 0.014$
CDF	$0.176 \pm 0.031 \pm 0.032$
ALEPH	$0.132 \pm 0.022^{+0.015}_{-0.012}$
OPAL	$0.145^{+0.041}_{-0.035} \pm 0.018$
L3	$0.110 \pm 0.019 \pm 0.015$
Average [72]	0.148 ± 0.018

Table 11: Results for $\chi = f_d\chi_d + f_s\chi_s$.

In order to relate the mixing results from LEP and from the hadron colliders to the mixing results from the $\Upsilon(4S)$, one must make some assumptions about f_d and f_s. In Fig. 24, taken from ref. [72], the mixing parameters χ_s and χ_d are plotted on the x and y axes, respectively. A band at constant

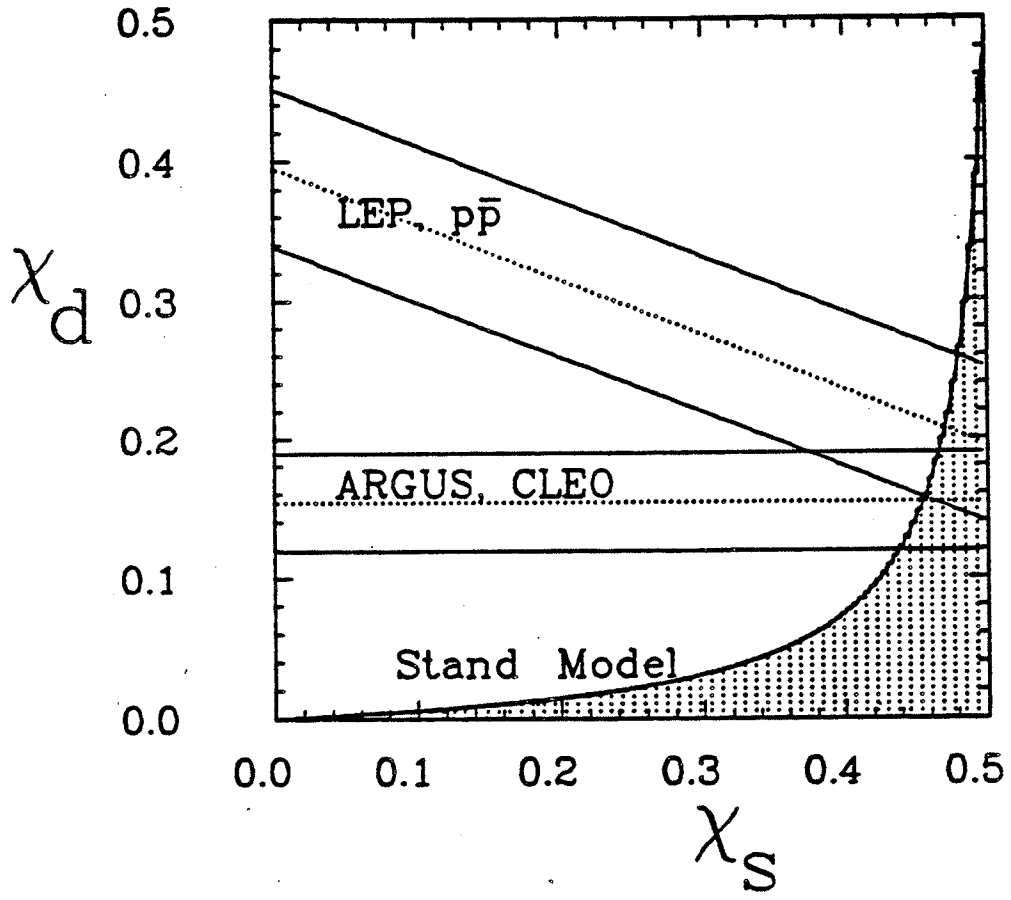

Figure 24: Experimental constraints on χ_d and χ_s, and the Standard Model prediction assuming unitarity of the CKM matrix (shaded region), from ref. [72].

χ_d shows the constraints from the mixing measurements of B_d mesons performed on the $\Upsilon(4S)$, while the diagonal band shows the constraint from the LEP and $p\bar{p}$ machines, assuming $f_d = 0.375$ and $f_s = 0.15$. The two measurements are in serious disagreement if we assume χ_s=0, and this provides us with strong, though indirect, evidence for the B_s. The shaded region shows the allowed values in the Standard Model which are derived from unitarity of the CKM matrix. The intersection of all three is a fairly small area which is very close to $\chi_s = 0.5$, as we expect from the estimate we made earlier.

As χ_s approaches 0.5, the precision with which x_s is determined using dilepton events deteriorates rapidly. At most one can hope to set a lower limit. From the Fig. 24 the intersection of the 1σ bands occurs at around $\chi_s = 0.37$, from which we can set the limit $x_s > 1.7$, which is a rather weak limit. Instead, a different technique is necessary in which the oscillation frequency, characterized by ΔM, is directly determined by measuring the decay length and tagging the decay as a B_s or $\bar{B}_s$. This is experimentally much more difficult than measuring the rate of dilepton events and will require very high statistics as well as precision vertex tracking.

4.6 The B_s and the Λ_b

Although the B_s has not technically been 'discovered', in the sense that its mass has not yet been determined, there is indirect evidence for its existence from mixing measurements. Recently there has been additional evidence for its production in Z^0 decays. The ALEPH and DELPHI experiments have used partial reconstruction to tag B_s decays using events in which a D_s and a high p_t lepton were reconstructed in the same jet. There is also B_s production from B_d and B_u decays, with an inclusive rate of around 11%. However this process is dominated by the spectator decay diagram in which $W \rightarrow c\bar{s}$. Therefore it is unlikely that a high p_t lepton will be produced in association with a D_s which originates from a B_d or B_u. ALEPH [78] reconstructs the D_s in the $\phi\pi^-$ or $K^{*0}K^-$ mode, reporting a signal of 17.0 ± 4.5 events, corresponding to a product branching ratio $Br(\bar{b} \rightarrow B_s \rightarrow D_s^- X l^+ \nu)$ of $0.04 \pm 0.011^{+-.010}_{-0.012}$. They have not yet officially reported a lifetime based on the impact paramter of the observed leptons. DELPHI [79] has observed 7 candidates with a D_s reconstructed in the $\phi\pi^-$ final state, associated with a high p_t muon. Based on these limited statistics they quote the ratio of the B_s lifetime to the average B hadron lifetime as 0.8 ± 0.4.

Evidence for the Λ_b has been reported by the UA1 collaboration [80] in $p\bar{p}$ collisions at $\sqrt{s} = 630$ GeV. They report a signal of 16 ± 5 Λ_b's above a background of 9 ± 1 events. The Λ_b is reconstructed in its decay to $J/\psi\Lambda$, and the mass is measured to be $5640 \pm 50 \pm 30$ MeV/c^2; see Fig. 25. OPAL [81]

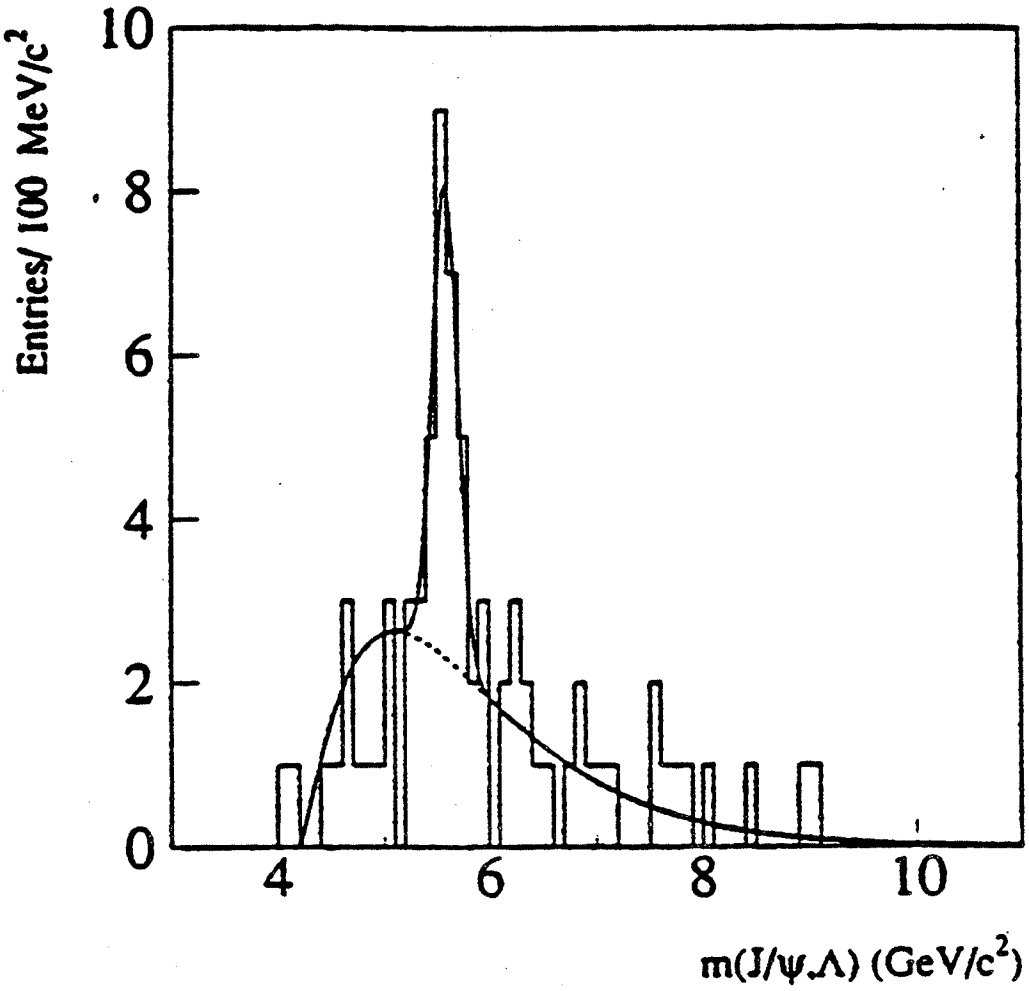

Figure 25: Invariant mass distribution of reconstructed $\Lambda J/\psi$ events, from the UA1 experiment (ref. [80]).

and ALEPH [82] have also claimed evidence for Λ_b production in Z^0 decays, both looking at Λl^- correlations. ALEPH has reported a lifetime for beauty baryons of $1.12^{+0.32}_{-0.29} \pm 0.15$ ps using the impact paramter distribution of the 122 leptons in their sample. This lifetime is averaged over all beauty baryons which decay semileptonically to a Λ, which may include a whole spectrum of states.

5 Future Prospects for B Physics

In the near future we can look forward to new results in many areas of B physics. Both CLEOII and ARGUS are now running, and the huge statistics that CLEOII is accumulating should have a particularly big impact on the field. There are many statistics-limited analyses which can be improved, such as the determination of exclusive branching fraction, measurement of meson masses, extraction of $|V_{ub}|$, search for rare decays and so on. In addition to these physics results, one hopes that the 'engineering numbers', the fraction of non-$B\bar{B}$ decays of the $\Upsilon(4S)$ and the ratio of charged to neutral B meson production, will also become more precise. The long-term plans for CESR are to continue upgrading the luminosity, with the eventual goal of reaching 1×10^{33} cm^{-2} s^{-1}. The production rate would then reach 24 million B's per year, as indicated in Table 12.

At LEP we have just had a hint of the B physics results which will be forthcoming as soon as the present run is analyzed. It is hoped that each experiment will log 1×10^6 Z^0's, which would be twice the previous data set. Given that three of the four experiments now have installed silicon vertex detectors, new lifetime measurements are likely. Flavor-tagged lifetime measurements of the B_d, B_u and B_s, and baryonic B's, are also possible though with much larger errors. It would be very nice if the production fraction of different B flavors could be determined, allowing the mixing measurements to be more easily interpreted. However this is complicated for the B_s by the fact that its branching fractions have not been determined. Measuring the masses of the B_s and Λ_b will be difficult but perhaps in another year or two sufficient statistics will have accumulated. At some point LEP will be upgraded to higher c.m. energy in order to explore physics above the W^+W^- threshold; however there has also been talk of upgrading LEP to a higher luminosity and continuing to run on the Z^0. This option, which I have called LEPII in Table 12, would make LEP into a B factory capable of producing 10 million B's per year.

In the areas of B spectroscopy and lifetime measurements, LEP will be competing with the Tevatron and in particular with the CDF experiment.

Machine	$\sqrt{s}$	$L, cm^{-2}s^{-1}$	$\sigma_{b\bar{b}}$	$\sigma_{b\bar{b}}/\sigma_{tot}$	b's $/10^7 s$
CESR II	10 GeV	1×10^{33}	1.2 nb	1/ 4	2.4×10^7
ABF	10 GeV	3×10^{33}	1.2 nb	1/ 4	7.2×10^7
LEP II	90 GeV	1×10^{32}	5 nb	1/ 5	1×10^7
TevII	2 TeV	5×10^{31}	50 μb	1/1000	5×10^{10}
SSC	40 TeV	1×10^{33}	500 μb	1/200	1×10^{13}

Table 12. B production at future e^+e^- and $p\bar{p}$ colliders.

CDF has also installed a silicon vertex detector and is actively pursuing many B physics analyses. The Tevatron is also starting a new run now, with the D0 experiment joining CDF for the first time. An integrated luminosity of 100 pb^{-1} is expected over the course of the next two years, 20 times the data set accumulated by CDF in the last run. D0 should also contribute with some new results on B production properties and on $B\bar{B}$ mixing, using their large magnetized muon system.

Looking even further ahead, there is an approved project at Fermilab to upgrade the Tevatron with a new Main Injector which will increase the luminosity to 5×10^{31} cm^{-2} s^{-1}, implying the production of about 50 billion B's per year. Both D0 and CDF have major upgrade plans which will enable them to pursue a serious program of B physics. The D0 upgrade proposal includes the addition of a solenoidal magnetic field, a silicon vertex detector, and improved tracking, all of which will make it more competitive in B physics. The most important goals for D0 and CDF include the measurement of B_s mixing by directly observing the oscillation rate, and the observation of CP violation. These goals are very ambitious, but the raw rates which are necessary are certainly there. The challenge will be to achieve sufficiently high trigger and reconstruction efficiencies.

Considering just the rates, it looks like the best future hope for B physics may be at the SSC where 10 *trillion* B's could be produced per year, at the design luminosity of 1×10^{33} cm^{-2} s^{-1} and the predicted total $b\bar{b}$ cross section of 500 μb. The signal-to-noise ratio of 1:200 is also much better than one finds at the Tevatron. No one has actually designed a B physics experiment that can use the full rate at the SSC, but it is a subject which is generating some interest already.

The other great hope for future studies in B physics is the asymmetric B factory. This new type of accelerator, first proposed by Oddone[83], combines the best features of the $\Upsilon(4S)$ with the big advantage one has in the continuum or on the Z^0, namely, moving B's. The idea is to operate with a c.m. energy equal to the $\Upsilon(4S)$ mass, but produced with unequal energy beams so that the $\Upsilon(4S)$ is moving forward in the lab frame. The B's will then be boosted and it will be possible to reconstruct the decay vertex of each B and measure the decay time. This has very important ramifications for CP violation measurements, because if one cannot measure the decay times on the $\Upsilon(4S)$, the CP asymmetries integrate to zero. At least 4 proposals have been made at various laboratories around the world to build such a device to study CP violation, and two of them, one here at SLAC[84] and the other at KEK[85], have a good chance to be approved.

So, to summarize, B physics is alive and flourishing at accelerators all around the world. A new wave of results is on the way from CLEOII, LEP

and the Tevatron, and future upgrades of these machines may keep us awash in B's for some time to come. In the more distant future we look forward to seeing B physics explored at the SSC, and to the construction of an asymmetric B factory.

6 Acknowledgements

I would like to thank Pier Oddone and Kam Biu Luk for carefully reading the manuscript and making constructive comments. Many thanks are also due to Glenda Fish and Lonnette Robinson for their help in the preparation of the manuscript and figures.

References

[1] E. Fernandez, *et. al.*, Phys. Rev. Lett. **51** (1983) 1022; N. Lockyer, *et. al.*, Phys. Rev. Lett. **51** (1983) 1316.

[2] C. Albajar, *et. al.*, Phys. Lett. **B186** (1987) 247.

[3] H. Albrecht, *et. al.*, Phys. Lett. **B192** (1987) 245.

[4] G. C. Fox and S. Wolfram, Phys. Rev. Lett. **41** (1978) 1581.

[5] J.D. Bjorken and S.J. Brodsky, Phys. Rev. **D1** (1970) 1416.

[6] E. Farhi, Phys. Rev. Lett. **39** (1977) 1587.

[7] H. Lipkin, Phys. Lett. **B179** (1986) 278.

[8] C. Bebek, *et. al.*, Phys. Rev. **D36** (1987) 1289.

[9] J. Alexander, *et. al.*, Phys. Rev. Lett. **64** (1990) 2226.

[10] M. Danilov, in *Z^0 Physics, Proceedings of the XXVth Rencontre de Moriond*, Editions Frontiers, France (1990).

[11] R. Poling, in *Proceedings of the Joint International Lepton-Photon Symposium*, ed. Hegarty, Potter and Quercigh, World Scientific, Singapore (1992).

[12] N. Byers and E. Eichten, Phys. Rev. **D42** (1990) 3885.

[13] G.P.Lepage, Phys. Rev. **D42** (1990) 3251.

[14] D. Atwood and W.J. Marciano, Phys. Rev. **D41** (1990) 1736.

[15] Y. Kubota, *et. al.*, NIM **A320** (1992) 66.

[16] H. Albrecht, *et. al.*, NIM **A275** (1989) 1.

[17] P. Abreu, *et. al.*, Phys. Lett. **B281** (1992) 383.

[18] 1992 Review of Particle Properties, Phys. Rev. **D45** (1992) 1.

[19] C. Peterson, *et. al.*, Phys. Rev. **D27** (1983) 105.

[20] B. Adeva, *et. al.*, Phys. Lett. **B261** (1991) 177.

[21] W. B. Atwood, SLAC-PUB-4827 (Dec. 1988).

[22] D.C. Hom, *et. al.*, Phys. Rev. Lett. **36** (1976) 1236.

[23] S.W. Herb, *et. al.*, Phys. Rev. Lett. **39** (1977) 252.

[24] P. Nason, S. Dawson, and R.K. Ellis, Nuc. Phys. **B303** (1988) 607.

[25] E. Berger, in *Proc. of the XXIVth Int. Conf. on High Energy Physics*, ed. R. Koffhaus and J. Kuhn, Springer-Verlag (1989) 987.

[26] M.G. Catanesi, *et. al.*, Phys. Lett. **B231** (1989) 328.

[27] C. Angelini,*et. al.*, NIM **A289** (1990) 342.

[28] J. Wiss, *et. al.*, Nuc.Phys.**B27** (1992) 207.

[29] P. Bordalo, *et. al.*, Z.Phys.**C39** (1978) 7.

[30] K. Kodama, *et. al.*, DPNU-92-37 (Aug. 1992) Submitted to Prog.Theor.Phys.

[31] P. Nason, S. Dawson, and R.K. Ellis, Nuc. Phys. **B327** (1989) 49.

[32] R.K. Ellis and P. Nason, Nuc. Phys. **B312** (1989) 551.

[33] D. Kuebel, *et. al.*, Phys. Rev. **D43** (1991) 767.

[34] E. Berger and R. Meng, ANL-HEP-PR-92-11 (Jan. 1992).

[35] E. Berger and R. Meng, Phys.Rev.**D46** (1992) 169.

[36] E. Berger, R. Meng and W. Tung , Phys. Rev. **D46** (1992) R1895.

[37] D. Baden, in *Proc. of the 18th SLAC Summer Institute*, ed. J. Hawthorne (1990) 489.

[38] E.W.N. Glover, A.D. Martin, and W.J. Stirling, Z.Phys.**C38** (1988) 473.

[39] C. Albajar, *et. al.*, Phys.Let.**B256** (1991) 112.

[40] C. Albajar, *et. al.*, Phys.Let.**B256** (1991) 121.

[41] F. Abe, *et. al.*, Phys. Rev. Lett. **68** (1992) 3403.

[42] K. Berkelman and S. Stone, Ann Rev. Nuc. Sci. **41** (1991) 1.

[43] H. Albrecht, *et. al.*,Z. Phys. **C48** (1990) 543.

[44] D. Bortoletto, *et. al.*, Phys. Rev. **D45** (1992) 21.

[45] D. Flamm, *et. al.*, Nuovo Cimento **98** (1987) 559.

[46] R.A. Ong, Ph.D. thesis, SLAC-0320, Sept. 1987.

[47] D. Decamp, . *et. al.*, Phys. Lett. **B257** (1991) 492.

[48] D. Buskulic, *et. al.*, Phys. Lett. **B295** (1992) 174.

[49] S.R. Wagner, *et. al.*, Phys. Rev. Lett. **64** (1990) 1095.

[50] R. Fulton, *et. al.*, Phys. Rev. **D43** (1991) 651.

[51] H. Albrecht, *et. al.*, Phys. Lett. **B232** (1989) 554.

[52] G. Altarelli, it et. al., Nuc. Phys. **B208** (1982) 365.

[53] Grinstein, it et. al., Phys. Rev. **D39** (1989) 799.

[54] Wirbel, it et. al., Z. Phys. **C29** (1985) 637.

[55] Wirbel, it et. al., Z. Phys. **C29** (1985) 269.

[56] Korner and Schuler, Z. Phys. **C38** (1988) 511.

[57] N. Isgur and M. Wise, Phys. Lett. **B232** (1990) 113.

[58] S. Henderson, *et. al.*, Phys. Rev. **D45** (1992) 2212.

[59] H. Albrecht, *et. al.*, Phys. Lett. **B249** (1990) 359.

[60] K. Wachs, *et. al.*, Z. Phys. **C42** (1989) 33.

[61] G. Altarelli and S. Petrarca, Phys. Lett. **B261** (1991) 303.

[62] R. Fulton, *et. al.*, Phys. Rev. Lett. **64** (1990) 16.

[63] H. Albrecht, *et. al.*, Phys. Lett. **B234** (1990) 409.

[64] H. Albrecht, *et. al.*, Phys. Lett. **B255** (1990) 297.

[65] R. Fulton, *et. al.*, Phys. Rev. Lett. **63** (1989) 651.

[66] H. Albrecht, *et. al.*, Phys. Lett. **B197** (1987) 452.

[67] H. Albrecht, *et. al.*, Phys. Lett. **B219** (1989) 121.

[68] H. Albrecht, *et. al.*, Phys. Lett. **B229** (1989) 175.

[69] H. Albrecht, *et. al.*, Phys. Lett. **B275** (1992) 195.

[70] H. Albrecht, *et. al.*, Phys. Lett. **B192** (1987) 245.

[71] M. Artuso, *et. al.*, Phys. Rev. Lett. **62** (1989) 2233.

[72] H. Schroder, in *B Decays*, ed. S. Stone World Scientific, Singapore (1992) 292.

[73] H. Albrecht, *et. al.*, Phys. Lett. **B229** (1989) 175.

[74] D. Decamp, *et. al.*, Phys. Lett. **B258** (1991) 236.

[75] P. D. Acton, *et. al.*, Phys. Lett. **B276** (1992) 379.

[76] C. Albajar, *et. al.*, Phys. Lett. **B262** (1991) 171.

[77] F. Abe, *et. al.*, Phys. Rev. Lett. **24** (1991) 3351.

[78] D. Buskulic, *et. al.*, Phys. Lett. **B294** (1992) 145.

[79] P. Abreu, *et. al.*, Phys. Lett. **B289** (1992) 199.

[80] C. Albajar, *et. al.*, Phys.Let.**B273** (1991) 540.

[81] P.D. Acton, *et. al.*, Phys. Lett. **B281** (1992) 394.

[82] D. Buskulic, *et. al.*, CERN-PPE/92-138, submitted to Phys. Lett. **B**.

[83] P. Oddone, in *Proceedings of the UCLA Workshop: Linear Collider $B\bar{B}$ Factory Conceptual Design*, ed. D. Stork, World Scientific, Singapore (1987) 243.

[84] 'The Physics Program of a High-Luminosity Asymmetric B Factory at SLAC', SLAC-353 (Oct. 1989); 'An Asymmetric B Factory Based on PEP', SLAC-372 (Feb. 1991); 'Workshop on Physics and Detector Issues', SLAC-373 (March, 1991).

[85] 'Progress Report on Physics and Detector at KEK Asymmetric B Factory', KEK Report 92-3 (May 1992).